

AN INTERFEROMETRIC STUDY OF A METAL SURFACE
UNDER DISTORTION AND IMPACT.

T
BF
Hol
603,322
Aug 62

Thesis presented to
The University of London
for the degree of
Doctor of Philosophy
by
JAMES HOLDEN
1951

ProQuest Number: 10096567

All rights reserved

INFORMATION TO ALL USERS

The quality of this reproduction is dependent upon the quality of the copy submitted.

In the unlikely event that the author did not send a complete manuscript and there are missing pages, these will be noted. Also, if material had to be removed, a note will indicate the deletion.



ProQuest 10096567

Published by ProQuest LLC(2016). Copyright of the Dissertation is held by the Author.

All rights reserved.

This work is protected against unauthorized copying under Title 17, United States Code.
Microform Edition © ProQuest LLC.

ProQuest LLC
789 East Eisenhower Parkway
P.O. Box 1346
Ann Arbor, MI 48106-1346

C O N T E N T S

Chapter		Page
I	The Optical Characteristics of the Features on a Deformed Metal Surface; The need for a Technique of Measurement.	I
II	Application of Interferometry to an Opaque Surface; Investigation of the Intensity Distribution within the Reflected Fringe System.	9
III	The Use of Reflection Fringes in Topographical Studies; The choice of Reflection Coefficients.	27
IV	The Use of Reflection Fringes in Topographical Studies; New Criterion of Resolution.	38
V	Introduction to the Experiments on Slip and Twinning	49
VI	Method for the Determination of Twinning Elements.	58
VII	The Twinning of Antimony and Bismuth Crystals.	74
VIII	The Twinning of Single Crystals of Zinc with Particular Reference to the Shape of the Twin Region	96
IX	Further Observations on Twinning and Discussion.	106
X	Observations upon the Formation and Development of Glide Bands - (I) Aluminium Crystals.	121
XI	Further Interferometric Measurements on Glide Bands in Aluminium Crystals.	141
XII	Discussion of experimental observations on Glide Bands in Aluminium Crystals.	152

ABSTRACT.

The conditions of use of interference fringes for topographical measurement of metal surfaces are investigated. The optimum conditions of the factors which are involved in the formation of fringe systems in reflexion and which control the sharpness and contrast of the fringes are determined. The limits of resolution of the interference method are discussed with relation to the scale of the surface deformation structures of typical metal crystals.

The mechanical twinning of suitably shaped single crystals of Bi, Sb and Sn is investigated and the interferometric measurements of the macroscopic shear of the specimens allows a full determination of the twinning elements involved. These goniometric measurements are pursued to the microscopic scale and thus attention is drawn to the shape of the initial region of twinning and its development; the observations being interpreted against the background of the elastic anisotropy of the metal crystals.

Measurements are made upon the phenomenon of slip by way of the slip bands produced on crystals of Aluminium subject to shearing stress up to 1 kgm. mm^{-2} . The commencement of the translation involved in the formation of surface steps is found to be very rapid but the bands subsequently develop by a more gradual process accompanied by movement of the lamellae between active slip bands; the small angles of tilt involved being measured by means of fringes. The measurements in conjunction with a dislocation model of slip yield quantitative data.

Chapter I

The Optical Characteristics of the Features on a Deformed Metal Surface; The Need for a Technique of Measurement.

The use of the optical microscope in the study of metals became usual after 1864 when a conventional method of preparation of the metal specimen of general application was introduced. By the end of the century, in the hands of workers such as Ormond and Rosenhain, the instrument revealed phenomena during the deformation of a metal by mechanical stress which were at once simple and striking and their fundamental nature remains.

The conventional preparation of the metal specimen in these studies was to bring the metal surface to a high polish, after previously being ground flat by fine abrasives, so that the initial surface was entirely featureless under the microscope, being everywhere in the case of a pure metal, of the same absorption, refractive index and colour. Subsequent stressing of the specimen while under observation reveals structure on the surface which must be due to relative movement of the metal surface since it is still everywhere optically homogeneous. Now such structure by its nature is not simply revealed in its early stages by the microscope working in a normal manner nor is the microscopic image to be easily interpreted quantitatively. In perhaps the first metallographic observations of this kind, G. Charpy (1896), comments upon his method of revealing the surface structure of a polished specimen subject to a slight permanent deformation in a revealing manner:-

"mais elles ne sont visibles que dans certaines conditions; le meilleur procédé consiste à examiner les surfaces au microscope, en éclairant verticalement, de préférence avec l'oculaire éclairant de M. Cornu, et employant

"un objectif très faible, le grossissement se faisant par l'oculaire. Dans ces conditions il se produit des jeux d'ombre et de lumière que mettent en évidence de légères déformations de la surface".

Later observers without the great optical tradition of M.Charpy's times and background have not been so conscious as to the difficulties of rendering visible and interpreting the small "phase" details found on a deformed polished surface, and to the present day we have been dependent upon the principle "des jeux d'ombre et de lumière" to give us information about deformation structures using the optical microscope instead of being able to use the instrument for precise, quantitative observation.

Of recent years Zernicke has taken steps to develop the wave theory of the image formation of the small phase details, such as we are discussing in relation to the phenomena of metallic deformation. He has introduced the exact methods of phase contrast microscopy which enable us to produce a "true" image of the phase details on the object i.e. an image in which changes of intensity can be uniquely related to changes in refractive index or thickness in the object, and thus offers in principle a method of measurement of the topography of a deformed metal surface. In application, the carefully developed methods of Zernicke have found great use in the Biological field clarifying a wealth of hitherto obscure detail, similarly in relation to the surface structures of deformed metal specimens the technique by means of its properties of contrast produces accurately focussed images, but the possibility of obtaining exact measurements from the images has not been achieved, nor does it appear likely as will presently be discussed.

It is in this matter of measurement that the needs of studies in metal physics are most felt and to investigate further we must ask what is the scale of the phase details

produced by deformation under controlled conditions and what are the inherent difficulties of present optical techniques as regards measurement?

Figure I represents schematically the typical scale of some important etching and deformation details which optical and other techniques have indicated on metal surfaces, originally polished.

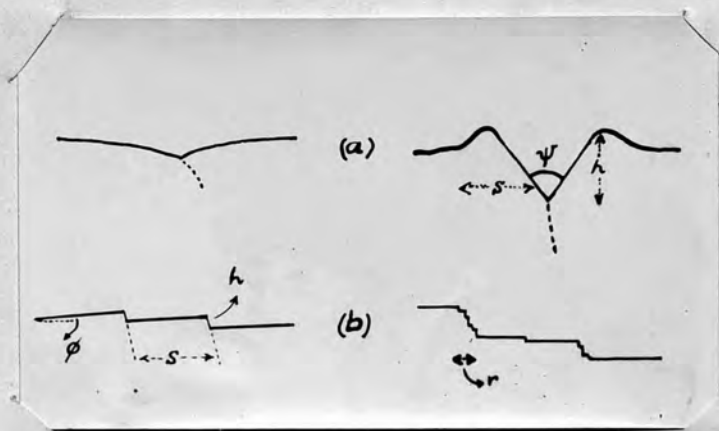


Figure I.

A section through a boundary between two grains is shown in (a), the lettered diagram represents the development of the boundary by thermal etching where " h " $\sim 10^{-4}$ cms. and " s " $\sim 10^{-4}$ cms. A section through a system of slip bands is shown in (b). In this case at the beginning of a deformation " s " may be of the order of millimetres while " h " is less than 10^{-6} cms. At a later stage of the deformation " s " may be reduced to 10^{-4} cms and " h " developed to $2 \cdot 10^{-5}$ cms., or, alternatively as the second part of the diagram represents inside a region " r " $\sim 10^{-4}$ cms. we may have a finer structure of steps each of the order of $2 \cdot 10^{-6}$ cms. In twinning movements and deformations which may involve the tilting of grains then we are interested in measuring angles such as ϕ which may be initially as small as 10^{-4} radians. Since the deformation is crystallographic the section represented is

repeated in a direction normal to the plane of the paper to give the three dimensional structure on the metal surface.

When deformation structures such as these are viewed under the microscope it is seen that none of them will modify the amplitude of the light falling upon them only the phase of the light reflected to form the image will be changed. Thus, recalling the Abbe theory of image formation, Figure 2, the diffraction spectra $I_0 : I_1 ; I_2 \dots$ will give rise to an image possessing differences in phase but of uniform intensity. In the image plane therefore the structure is invisible. This invisibility is however upset by any deviation from ideal conditions which will serve to disturb the exact balance of the different compounding vibrations, thus the invisibility is seldom achieved absolutely. The intentional deviations used to cause disturbance of intensity and thus render visible in the image plane something related to the structure of the object detail are as follows.

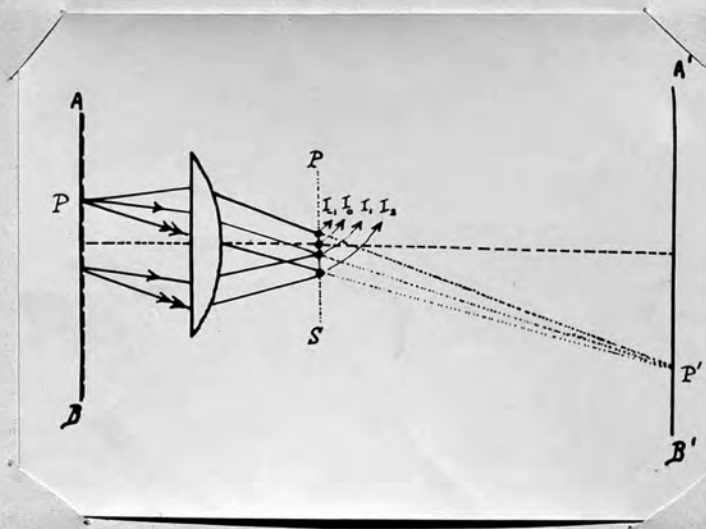


Figure 2

In Figure 2 we consider the metal surface AB with a periodic phase structure in parallel lines. We can intercept the spectra ($I_0:I_1:I_2\dots$), by having sufficiently oblique incident illumination so that only diffracted beams from the surface structure enter the objective. We then obtain the well known dark ground effect in which all contours appear bright and broadened. Another kind of dark ground effect is obtained by intercepting the central image I_0 only. (Spierer 1926). Alternatively we can allow the spectra ($I_0:I_1:I_2\dots$), to go on and form the image i.e. the spectra on one side of the axis are intercepted in the plane PS. The observer then obtains the impression that he sees an obliquely illuminated relief of the object surface, in it the sharp edges tend to be rounded off. (Toepler 1867).

The most widely used method of obtaining an image depends however on the fact that any changes in the relative phases of the spectra will cause intensity changes in the image giving a "detection" of structure in the object even though it is on a scale of only tens of Angstroms. This is a condition simply achieved by changing the focus of the microscope from the object surface i.e. changing the plane in which the interference to form the image is observed. This is perhaps done unconsciously in the examination of typically highly polished metal surfaces but it is to be appreciated that the graphic image of the surface thus obtained gives no clear idea of the unique detailed structure of the object. In the case of a surface with detail in slightly different planes the complexity of the method is readily seen since the degree to which we are employing the method is different for each plane and the structure is revealed to a different degree for each plane. Only in the limiting case of a structure of extreme simplicity, e.g. a single step, relatively isolated on a plane surface can we hope to attempt a quantitative measurement from the

method, and this is not easily arrived at in general. The sensitivity of the procedure is outstanding; using monochromatic illumination and stopping down the incident beam to a narrow pencil in a microscope system well corrected against glare, then a small step put down by thermal evaporation of silver onto a silvered optical flat and measured interferometrically as being less than 80 Angstroms high, can readily cause a disturbance in the image plane as we focus through the plane of the silver. For most of the surfaces of interest in metal physics the limitations mentioned above reduce the method to one of detection only.

The new method of changing the relative phases of the spectra is ^{the} phase contrast method of Zernicke and is based upon the wave theory. A known path difference of $\frac{\lambda}{4}$ is introduced between the spectra and the central image, I_0 , by the employment of a correctly designed and located "phase-plate". The resultant image is thus produced under known conditions and can be interpreted; however, in the case of a typical metal structure the quantitative measurement of the changes in intensity of various parts of the image cannot be taken to an exact degree since in any practical arrangement there are contributions of intensity in the region of the detail under examination from contiguous portions of the surface.

With the method of phase contrast microscopy stopping short of the stage of precise measurement, and possessed of the exhaustive work of Zernicke on the wave theory of image formation, the search for a method of measuring the topography of small phase details on a metal surface must take a new turn. Our difficulties so far are caused by the attempt to represent by a variation of intensity in two dimensions, the three dimensional topography of the metal surface. This appears unnecessarily ambitious when it is remembered that the structures caused by deformation, being crystallographic, tend to have a line form and occur

on a surface prepared to a uniform finish. Thus a technique that will represent a two dimensional section of the metal surface in the two dimensional image plane, by means of intensity variations, will be adequate for our purposes as long as we can scan the surface, taking in different sections. This method of representation is found in the use of interference fringes to be formed by the surface.

The methods of interferometry¹ have been used to study the transparent surfaces of Diamond, Mica and Calcite. The crystal surface, silvered to a high reflectivity is brought close to a silvered, optically flat, reference surface. The localized interference fringes formed in transmission by the interferometer thus formed are used to deduce the topography of the crystal surface. We must therefore investigate the application of this method to an opaque metal surface; when the reflected system of interference fringes will have to be used; and to the scale of the details which are formed in the deformed metal. The precision of measurement achieved in the case of the transparent crystals has been very high and the extension of the method to metals would greatly add to the already wide flexibility of the optical microscope as a tool of research in Metal Physics.

¹ For references, see p. 8.

References - Chapter I.

- Sorby.H.C., Brit.Assoc.Rep., 1864, 11, 189.
J.Iron Steel Inst., 1886, 1, 140.
- J.A.Ewing & W.Rosenhain., Phil.Trans., 1900, 193A, 353.
- G.Charpy., Comptes Rendues, 1896, 123, 226.
- F.Zernicke., Physica, 9, 1942, 686 & 974.
Mon.Not., 1934, 94, 377.
- E.Abbe., Arch.mikrosk.Anat., 1873, 2, 431.
- Toepler.A., Pogg.Ann., 1867, 131, 180.
- Spierer.C., Arch.sc.phys.nat., 1926, 8, 121.
- Tolansky.S.& Wilcock., Nature, 157, 583, 1946.
(Topography of the face of a Diamond Crystal).
- Tolansky.S.& Khamsavi.A., Nature, 157, 661, 1946.
(Cleavage of Calcite).
- Tolansky.S.& Morris.P.G.Min.Mag., XXVIII, 137, 1947.
(An Interferometric survey of the micas).

Chapter II

Application of Interferometry to an Opaque Surface; Investigation of the Intensity Distribution within the Reflected Fringe System.

Introduction.

The reflected system of interference fringes finds many applications, particularly in Metrology where the "Fizeau" localized fringes of equal thickness are most often used. However, a detailed investigation of the intensity distribution within the reflected system for the particular reflection coefficients involved appears to be confined to an early paper by Hamy^I, (1906), who showed several limiting conditions which the fringe intensity distribution could assume. In particular, with high reflection coefficients the intensity distribution could be made to vary quickly so as to give rise to very sharp fringes.

The work to be described in the present Chapter is an investigation of the reflected intensity distribution given by an interferometer whose reflecting surfaces are formed by thermal deposition of silver to various depths so as to form a full range of reflectivities from 4% to 92%. The interferometer is in the form of a wedge and the fringes of equal thickness localized on the zero order Feussner surface are used for the observations. The observations of Hamy, made on chemically deposited reflectors, have been confirmed and extended. The fringes arising in the range of low reflectivities lead to the measurement of a phase quantity which enables the optical constants of silver in the form of thin films to be evaluated, while in the range of high reflection coefficients the conditions for the use of the fringes in topographical measurements of structures on opaque surfaces are discussed, insofar as the choice of reflection coefficients is concerned.

The Reflected Intensity from a Plane Parallel Sheet.

The case of a plane parallel air film between silvered optical flats is first considered. The theoretical properties of such a system can be tested experimentally by using a simple wedge interferometer if the wedge angle and separation are appropriately chosen.

Figure 3 illustrates the two reflecting planes with normally incident parallel light giving rise to families of reflected and transmitted wave fronts.

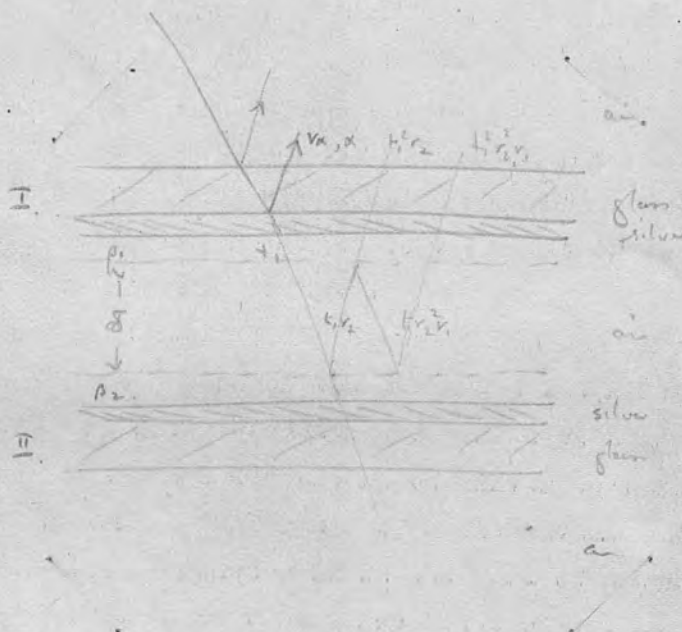


Figure 3.

Let the factors by which the amplitude of a plane wave is caused to change on reflection at the air/silver interface of reflectors I and 2 be r_1 and r_2 and let $\beta_1; \beta_2$ be the accompanying phase changes at these reflections. Let $r_\alpha; \alpha$ be the similar quantities for the reflection at the glass/silver interface of reflector I. Finally let $t_1; t_2$

be the amplitude transmission factors of the surfaces I and 2 and $\tau_1; \tau_2$ the phase changes at these transmissions. The changes of phase $\alpha; \beta_1; \beta_2$ are illustrated in a geometrical manner in the Figure, that is by assuming them equivalent to a change in air gap.

Assuming a plane wave of unit amplitude to be incident normally on the interferometer, the state of interference at any point X in the focal plane of a collecting lens is given by the vector sum of the disturbances due to each reflected wave. For the reflected system the resulting vibration at X is therefore given by:-

$$v_x = r_\alpha \cdot \cos(\theta - \alpha) + \sum_{n=1}^{\infty} t_1^2 \cdot r_2^n \cdot r_1^{n-1} \cdot \cos\left[(\theta - 2\tau_1) - \{(n-1)\beta_1 + n(\beta_2 + \delta)\}\right]$$

Assuming that the absorption is the same for each direction of transit of a surface; and the reflected intensity is thus:-

$$I_{R_x} = r_\alpha^2 + \left\{ \frac{(t_1^2 r_2^2)^2 + 2 t_1^2 r_2^2 r_\alpha \cdot \cos(\delta - \alpha + \beta_2 + 2\tau_1) - 2 t_1^2 r_2^2 r_1 r_\alpha \cdot \cos(2\tau_1 - \beta_1 - \alpha)}{1 + r_1^2 r_2^2 - 2 r_1 r_2 \cos(\beta_1 + \beta_2 + \delta)} \right\}$$

In the same nomenclature the transmitted intensity is:-

$$I_{T_x} = \left\{ \frac{t_1^2 \cdot t_2^2}{1 + r_1^2 r_2^2 - 2 r_1 r_2 \cos(\beta_1 + \beta_2 + \delta)} \right\}$$

The factor:-

$$\left(1 + r_1^2 r_2^2 - 2 r_1 r_2 \cos(\beta_1 + \beta_2 + \delta) \right)^{-1} = \mathcal{Q}_{\delta + \beta_1 + \beta_2}$$

is the term familiar in its role in the Fabry-Perot interferometer where advantage is taken of the rapid variation of $\mathcal{Q}_{\delta + \beta_1 + \beta_2}$ about $\beta_1 + \beta_2 + \delta = 2n\pi$ as $r_1 \cdot r_2 \rightarrow 1$.

Writing $(\delta + \beta_1 + \beta_2)$, the optical separation of the two surfaces, as Δ , the transmitted system may be written:-

$$I_{Tx} = \mathcal{O}_\Delta [t_1^2 t_2^2]$$

And the reflected system, observing that the phase quantity $(2\tau_1 - \beta_1 - \alpha)$ depends only on the phase conditions at the first surface, I, and is represented as "F":-

$$I_{Rx} = r_1^2 + \mathcal{O}_\Delta \left[(t_1^2 r_2^2) + 2t_1^2 r_1 r_2 \cos(\Delta + F) - 2t_1^2 r_2^2 r_1 \cos F' \right]$$

For the simplified case of a symmetrical interferometer where $r_1^2 = r_2^2 = R$, and $t_1^2 = t_2^2 = T$, the expressions become:-

$$I_{Tx} = \mathcal{O}_\Delta [T^2]$$

$$I_{Rx} = R + \mathcal{O}_\Delta \left[TR^2 + 2TR \cos(\Delta + F) - 2TR^2 \cos F' \right]$$

It is seen that while the transmitted system is described by an expression consisting of the function \mathcal{O}_Δ , (the Fabry-Perot "shape" function), multiplied by a magnitude term involving only the transmission factors of the two surfaces; the reflected system is quite different since in addition to a continuous background term, R, there are two transmission-like terms, one of which involves $\cos F$ in its magnitude, and also there is a term which is unique since it is out of phase with \mathcal{O}_Δ by an amount F.

We have, as yet, no experimental measurements of F, but we can derive the general condition leading to maxima and minima in the expression for the reflected intensity, I_{Rx} .

The condition leading to maxima and minima in reflection is:-

$$\sin \Delta \left(t_1^2 r_2^2 r_1 r_2 + r_1^2 r_2^2 r_1 \cos F - r_2^2 r_1^2 r_2 \cos F \right) + \cos \Delta \left(r_2^2 r_1^2 \sin F + r_1^2 r_2^2 r_1 \sin F \right) = 2 r_2^2 r_1^2 \sin F$$

Which may be written:-

$$m \sin \Delta + n \cos \Delta = p.$$

Where m, n and p are functions of r_1, r_2, r_α, t_1 and F . The solutions of the equation may be written:-

$$\Delta = 2n\pi + a.$$

$$\Delta = (2n+1)\pi + b.$$

Where one of the series of roots corresponds to maxima and the other to minima, the quantities a and b being of the order of π and dependent upon the values of r_1, r_2, r_α, t_1 and F , that is, upon the reflection coefficients of the two surfaces of the interferometer and upon the transmission coefficient and phase changes at the first or incident surface. Since the two series of roots will not in general be at equal intervals the reflected system will be expected to be asymmetrical.

The condition that the roots be equally spaced is that in the equation:-

$$\frac{\partial I_{R_x}}{\partial \Delta} = 0$$

the independent term, p , is zero, i.e.

$$2 r_2^2 r_1 r_\alpha \sin F = 0$$

Which can occur when:-

$$\sin F' = 0$$

Two cases can arise, namely:-

$$F = 2n\pi \dots\dots\dots (a)$$

$$F = (2n+1)\pi \dots\dots\dots (b)$$

In the first case, intensity maxima occur at $\Delta = 2n\pi$ and minima at $\Delta = (2n+1)\pi$. In the second case minima occur at $2n\pi - \Delta$ and maxima at $\Delta = (2n+1)\pi$.

The other limiting condition of the intensity distribution which arises from the form of the equation for maxima and minima in the reflected system, occurs when the two series of roots superimpose, i.e. when:-

$$m^2 + n^2 = p^2 \dots\dots\dots (c)$$

That is, when:-

$$\left. \begin{aligned} F' &= (2n+1)\pi \\ t_1^2 &= \frac{r_2^2 r_\alpha^2 (1 - r_1^2 r_2^2)}{r_2^2 r_1^2 r_2^2} \end{aligned} \right\}$$

Of these three conditions, cases (a) and (c) represent limits to which experimental conditions can tend while case (b) occurs when the incident reflecting surface, I, is an uncoated dielectric, e.g. glass, for which $r_I^2 = 0.04$, and $F = (2n+1)\pi$.

Extension to the case of a Wedge.

It has been shown in the case of a wedge, (Brossel, 1947)², that the phase of the n^{th} beam with respect to the direct in the case of the transmitted system is closely given by:-

$$\phi_n = n\delta - n^3 \frac{8\pi \cdot t \epsilon^2}{3\lambda}$$

As compared with $\phi_n = n\delta$ for strictly parallel surfaces, where ϵ is the wedge angle and t the wedge separation. In his examination of this phase relation Brossel finds that if the phase terms $n^3 \frac{8\pi \cdot t \epsilon^2}{3\lambda}$ are small the fringes are asymmetrical, as they become greater, secondary maxima (in the case of transmission), occur close to the main maxima which are of period $\frac{\lambda}{2}$. These considerations apply equally to the multiply reflected beams of the reflected system but the asymmetry due to this cause can be made negligibly small, so as not to confuse with the fringe asymmetry arising from the intrinsic phase characteristics of surface I, by the choice of an appropriate wedge angle, (ϵ), and order of interference, (t), thus making the phase lag terms due to the presence of the wedge angle negligibly small. The deductions made in the case of a parallel sheet thus apply to a wedge chosen in this way. The use of localized wedge fringes for an experimental investigation is most convenient and has the advantage over the use of fringes of equal inclination arising from a parallel sheet in that optical flats of high quality are not essential. For in the latter case irregularities in surface figure of the reflectors leads to fringe broadening since integration of the light from over the reflector surface takes place.

Experimental Arrangements.

The optical arrangement consists of a source arm complete with collimating system which can be moved with respect to a fixed wedge interferometer and viewing system so that the transmitted and reflected fringe systems localized on the Feussner surface of zero order can be in turn observed. Figure 4 illustrates this.

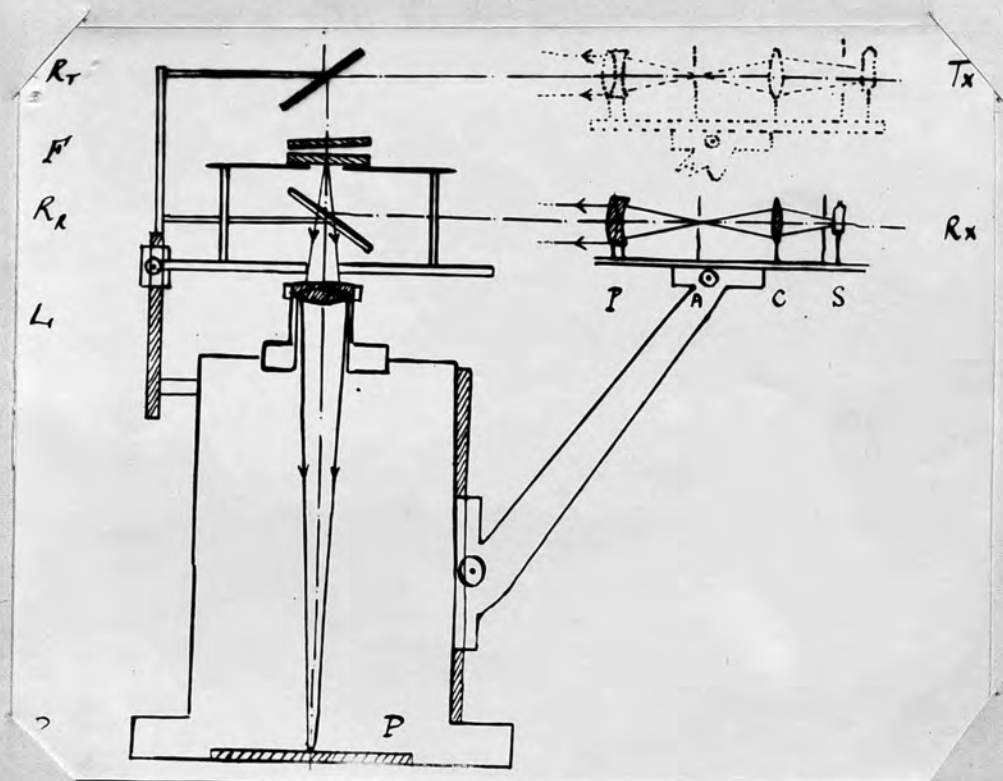


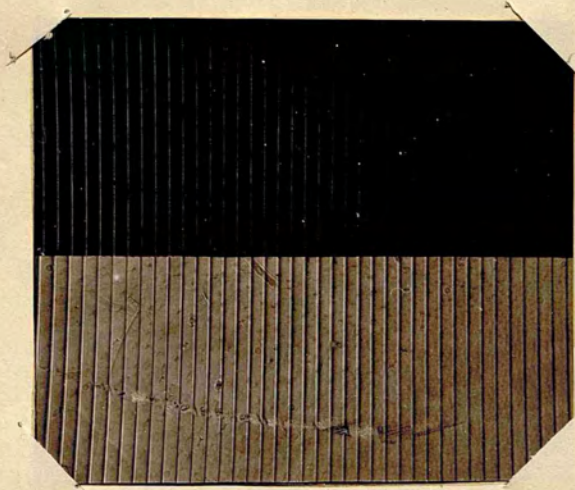
Figure 4.

Special attention must be given to the collimation and angle of incidence of the light in each of the two positions of illumination. It is observed experimentally that the reflected intensity distributions close to the Feussner surface of zero order, F_0 , have a markedly asymmetrical appearance with respect to the

appearance of the distribution on the Feussner surface itself. Focussing progressively away from the Feussner surface causes the asymmetry to quickly attain the appearance of an adjacent maximum and minimum against the background. Figure 5(a), shows the appearance of the reflected system, when the plane of focus is relatively steeply inclined to the Feussner surface, in the lower part of the photograph. The accompanying transmitted system, photographed on the same plate by means of a split shutter camera, under the same conditions, does not reveal its asymmetry at normal exposures. Over a small field and in the absence of any guide to focussing, such as fine rulings made by a razor blade on the silvered interferometer surfaces, this asymmetry will be confusing unless it can be made negligibly small. The distribution close to the surface F_0 has been studied in the case of multiple beams in transmission² and the following phase relation deduced:-

$$\phi_n = n\delta - n^2 \frac{4\pi X \epsilon^2}{\lambda}$$

Where ϕ_n is the phase of the n^{th} . reflected beam with respect to the direct at the point X; X being the distance, in the direction normal to the wedge, from the common line of the wedge. The wedge is of angle ϵ . This relation has the same general properties as the one described when considering the effects of wedge angle upon the fringes. It is therefore important, in an analogous way, to have X and ϵ such that the terms, $\left\{ n^2 \frac{4\pi X \epsilon^2}{\lambda} \right\}$, are negligibly small. This resolves into a condition of strict collimation of the incident light, since, if the incident light is collimated such that the angles of incidence are between the normal and a small



(a)



(b)

Figure 5.

angle θ , then the position of the Feussner surface, $(F_0)_\theta$ for the light incident at angle θ is:-

$$X_\theta = \frac{t}{\epsilon} \cdot \sin\theta$$

Where X_θ is the distance normal to the interferometer at a separation of t . (c.f. Figure 6). If the plane of focus coincides with Feussner surface, $(F_0)_0$, for the normally incident light, then it will be a distance $\frac{t}{\epsilon} \cdot \sin\theta$ from the surface $(F_0)_\theta$. Therefore θ must be chosen such that the terms:-

$$n \cdot \frac{4\pi X_\theta \cdot \epsilon^2}{\lambda}$$

are small compared with $n\delta$.

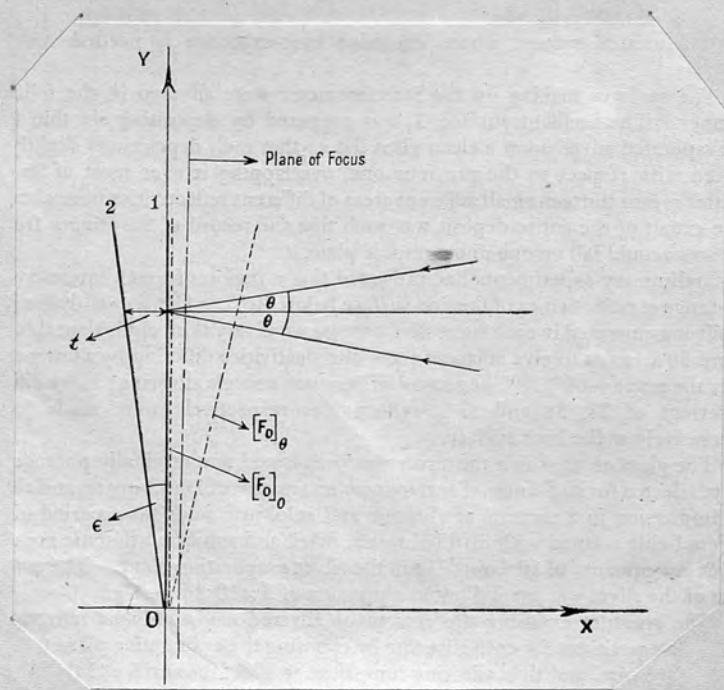


Figure 6.

Another reason why the collimation should be especially rigorous is that the incident beam has to illuminate the interferometer from two successive positions such that the transmission surface, $(F_0)_{Tx}$, and the reflection surface, $(F_0)_{Rx}$, are coincident within the same toleration as that discussed above for the Feussner surfaces within the one system. By using a long focal length collimating lens of 20cms. and a source aperture 1mm. in diameter θ was reduced to about $15'$. Using a wedge angle of less than $1'$ and working with an order of interference of less than 25 the focussing and wedge angle terms were made sufficiently small as to be negligible.

Finally the lens used for the observations must be of sufficient aperture to collect the multiply reflected emergent beams. The lens chosen was of Focal length 50mms., $f3.1$. Figure 5(a) shows the effects of using an inadequate lens. Apart from the curvature of the field, the point of interest interferometrically is the variation of the fringe shape along the length of the fringe due to the aperture of the lens being too small for the wedge angle used. In the the photograph the transmitted and reflected fringes from the wedge are seen together and it is clearly seen how much more obviously the errors of all kinds reveal themselves in the reflected system where the light intensity is high and the background level between the fringes is not close to zero, as in the transmitted system, for ordinary times of exposure as used in applications of interferometry.

In Figure 5(b) the breaking up of asymmetrical fringes into subsidiary maxima and minima, as described on p.15, is illustrated by means of reflected fringes from a wedge of extreme angle.

Interferometer Silverings.

The surface which made up the interferometer were silvered in the following manner. The surface I, the incident surface, was prepared by depositing six thin layers of thermally evaporated silver upon a small, clean glass flat such that each deposit was slightly displaced with respect to the previous one, overlapping it over most of its area. By this means thirteen small adjacent areas of different reflectivities were obtained. The extent of the entire deposit was such that the photographic record of the fringes from all the areas could be made on one plate.

Preliminary measurements had indicated that a region of much interest was in the range of reflectivities of the first surface below 30%. Consequently the layers of silver evaporated in each successive process were very thin, equivalent thickness about 50\AA , so as to give adjacent areas of reflectivities differing by a few per cent over the range 4-60%. The composite first surface silvering is indicated in Figure 7. The second, or back surface silvering, was a single layer; three different silverings of 28%, 58% & 87% being used in this position.

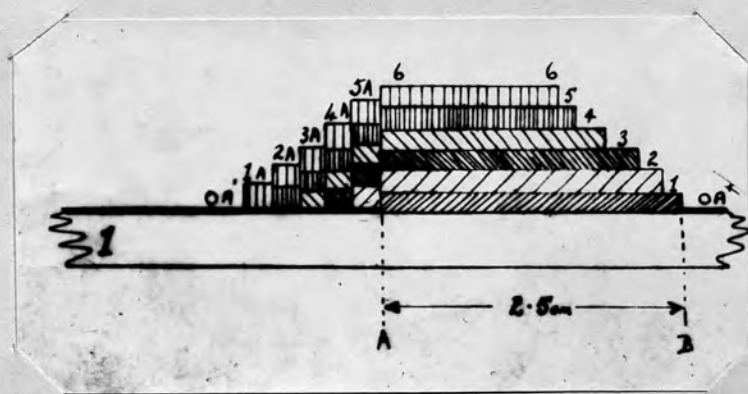


Figure 7.

The glass onto which the silver was evaporated was photographic plate selected for its flatness of surface over an area of about 1 cm.sq., and cleaned by immersion in a mixture of chromic and sulphuric acids for a period of days before being washed with distilled water, dried and subjected to ionic bombardment in the silver evaporation apparatus at a pressure of 10^{-2} mms.Hg. The actual evaporation of the silver was carried out at a pressure of $5 \cdot 10^{-4}$ mms.Hg.

The aperture exposing the area to be silvered could only be moved to its successive positions for each silvering by opening the ~~evaporation~~ evaporation apparatus to atmospheric pressure, and thus allowing the atmosphere to affect the surface of the silver between deposits. The silverings thus prepared were used in the interferometer within a few hours of their preparation, and no inconsistency in the observations due to possible changes in the films in this period were apparent. The thin silverings with reflection coefficients in the range 4-20% exhibited a striking range of colour both in reflection and transmission. The subtle colour changes being most evident when the films of different reflectivities were seen side by side as in the compound front surface silverings. Starting from the clear glass the thinnest films showed a very light straw colour in transmissi^{on} changing with increasing "thickness" to yellow, orange-yellow, orange, orange-red, purple, light blue and finally for films of greater reflectivity than 25% one sees the characteristic tones of dark blue of silver films, gradually darkening as the silver film increases in thickness to the limit of transmission at about 95% reflectivity.

Observations and Measurements.

Figure 8 shows the localized Fizeau fringes from a wedge interferometer whose incident surface was formed of six silverings to give areas of reflectivities 4, 7, 8, 11, 15, 23 and 58%, and whose back surface was formed of two silverings of reflectivities 28 and 58%, the field of view being so arranged that the seven areas on the front surface covered each of the different back surface areas. In the figure the reflected and transmitted systems are indicated by R and T respectively, with appropriate sub-scripts to denote the reflectivities of the front and back surfaces for the particular area involved, the incident surface being given first. In this particular compound silvering the final evaporation was rather heavy, bringing the maximum reflectivity of the area upon which it was deposited up to 58%; the second sequence of reflectivities on the surface was therefore in the reflectivity range 35 to 58%, a range which does not exhibit any large changes in F such as occur in the range 4 to 25%, and the fringes from these areas because of their sameness have been omitted from Figure 8.

The Figure thus shows the variation in intensity distribution of the fringes as the reflection coefficient of the first surface increases from 4 to 58%. With the aid of the transmitted fringes, which have the shape of gradually sharpening maxima as the reflectivities increase from left to right, and of the two vertical and one horizontal lines which are the images of fine scratches ruled onto the silver surface, it is easy to see the relative shift of the maxima and minima in the reflected system. When the first surface is un-coated glass ($r_1^2 = 0.04; F = (2n+1)\pi$), the reflected system shows minima coincident with the

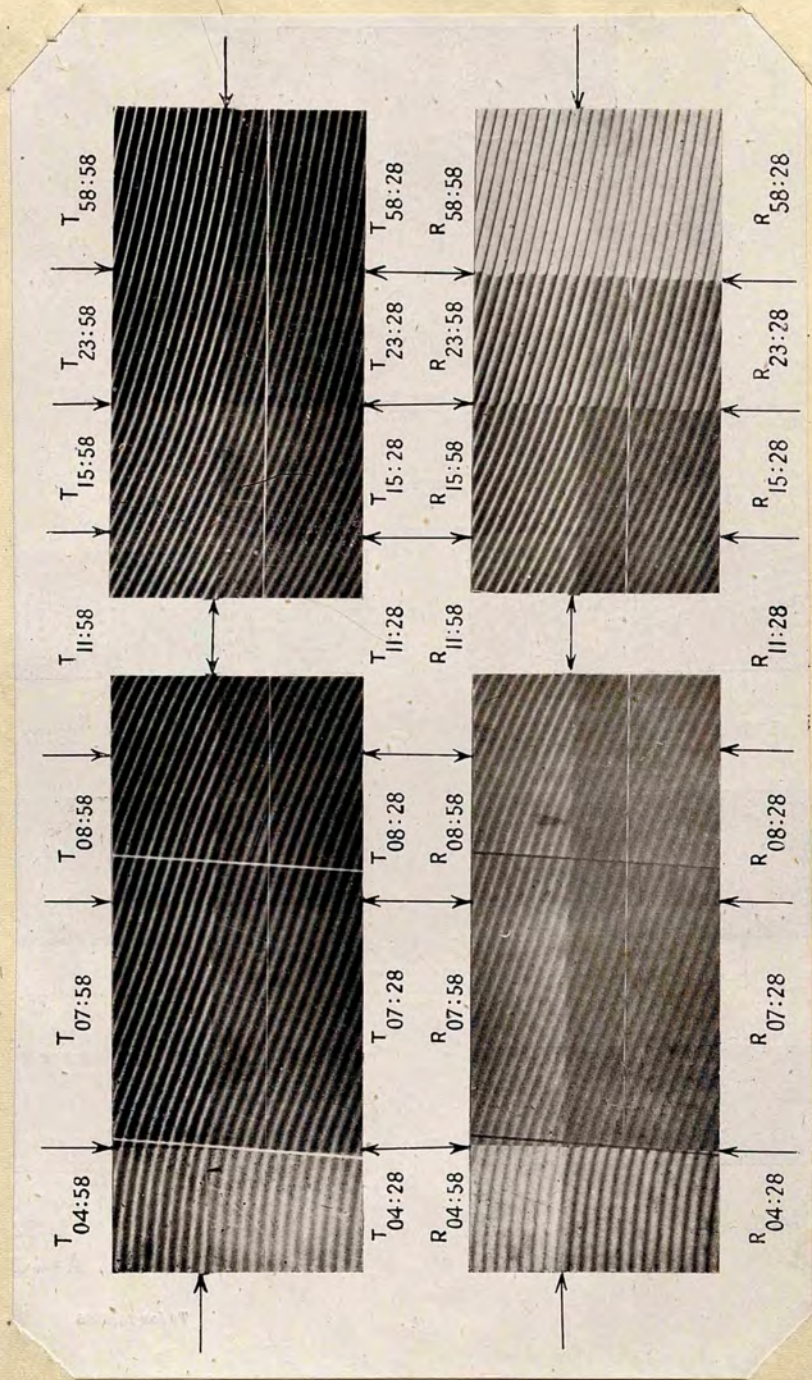


Figure 8

transmitted maxima. (The area $R_{04:58}$ is of some incidental interest in that the reflectors have greatly disparate reflectivities and yet the fringes are still easily visible). As the reflectivity of the first surface increases, the fringes go through a an asymmetrical sequence until at about 15% the reflected system shows sharp maxima almost coincident with the transmission maxima but much more luminous. (The relative times of exposure for the two systems from this area was 5:1). These fringes were first observed by Hamy (1906), and, noting their sharpness and high light efficiency he suggested their use in the examination of weak sources. He gave only a verbal description of the fringes and little attention seems to have been given to his experimental findings. The sharpness attainable by these "transmission-like" fringes is shown in Figure 9 (a), area $R_{15:87}$, wherein the back surface is made to have a high reflectivity approaching 90% and yet the light losses are due only to the double transit through the 15% reflecting silver film.

As the reflectivity of the first surface is still further increased, the fringes again become asymmetrical¹ the background intensity grows, and finally the visual appearance of the fringes is that of fine minima. Above 65% a microphotometer trace is needed to reveal the asymmetry, and above 85% this asymmetry due to the phase relations is so small as to be no longer certainly differentiated from that from other sources such as the small asymmetry due to the finite wedge angle and the small collimation defect.

Since, in Figure 8, the reflected fringes were recorded on the same plate as the transmitted fringes

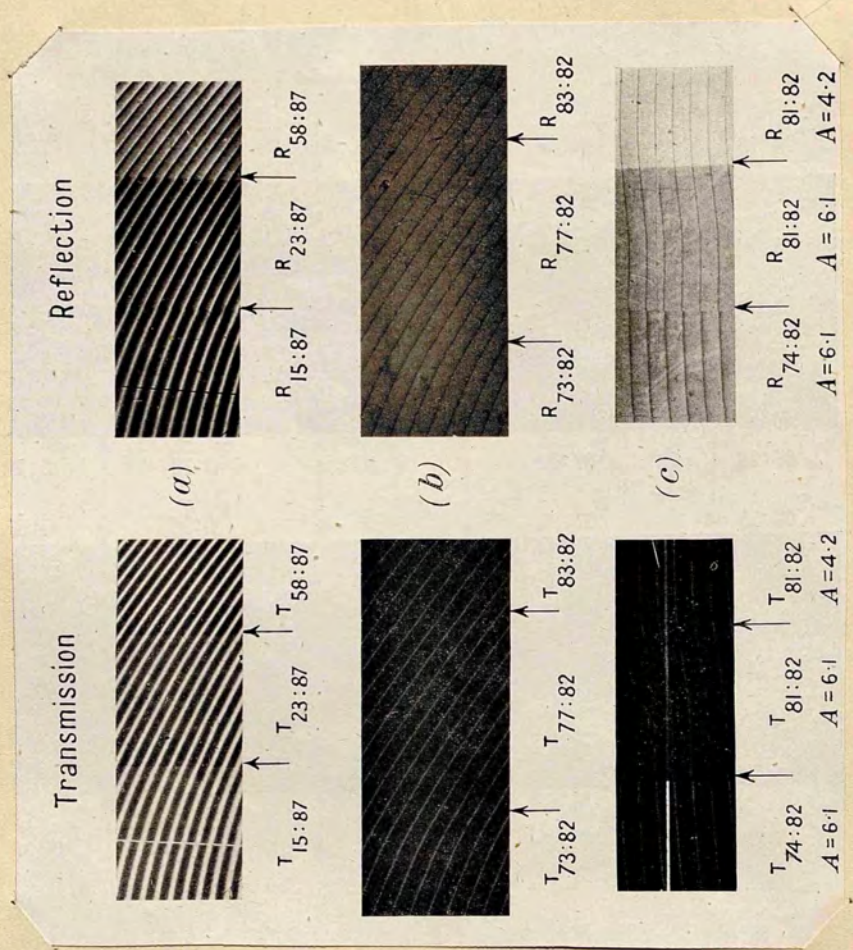


Figure 9

the relative intensity levels within the two systems from each area are roughly suggested. Figure 9(a) shows fringes from an interferometer made up of the same front surface as the upper right plate in Figure 8, but with a back surface of 87% reflectivity. The only effect of raising the reflectivity of the back surface is to sharpen all the fringes of the sequence while they retain their relative shapes, which are derived from the front surface conditions.

The transmitted and reflected fringes shown in Figure 8 were microphotometered using a photographic recording instrument. After determining the plate, (HP3), response characteristic the true fringe profiles were obtained, from which values of Δ satisfying the equation:-

$$\frac{\partial I_{R_x}}{\partial \Delta} = 0$$

were measured. Substitution of these values in the equation gives values of $F (= 2\gamma_1 - \beta_1 - \alpha)$. These are plotted in Figure 10 against an abscissa representing the reflection coefficients for the air/silver reflection at the front surfaces.

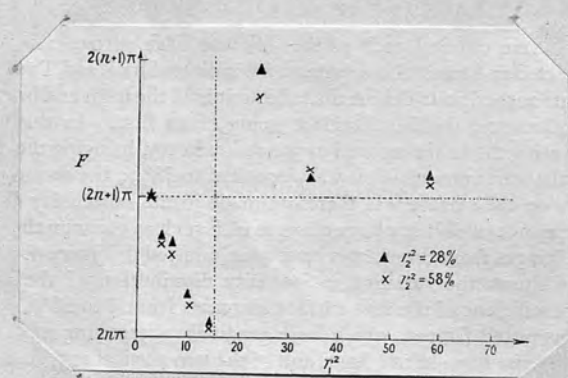


Figure 10

The reflectivities were measured by a Strong type reflectometer and checked by a graphical method employing the transmission fringe shape in conjunction with the equation expressing the intensity distribution in the transmitted system. The accuracy of measurement of r_I^2 fell to 2% in the range of reflectivities less than 40% while the accuracy of measurement of F was $\frac{\lambda}{30}$.

The experimental points in Figure 10 show a jump of 2π in the region of 15 to 20% reflectivity of the silver film. This is of interest and in the many reported investigations of silver films where the phase quantities α and β alone have been measured, some observers, (Rouard 1937), have noticed a jump in the values of α at very small thicknesses, but the experimental difficulties, (poor sharpness and visibility and sharpness of Fabry-Perot fringes in transmission at the low reflectivities of the thin films involved), are considerable. However, observation of the reflected fringe system from an interferometer, the front surface of which is the silver film under examination, immediately reveals in a clear manner the variation of the phase quantity F . From the discussion of the symmetry of the reflected fringes in Chapter I, the preceding experimental observations that the fringes change from symmetrical minima when the front surface is unsilvered through an asymmetrical minimum-maximum form and then become almost symmetrical maxima when the front surface is silvered to about 15%, means that F has changed from $(2n+1)\pi$ to $2n\pi$. As the reflectivity further increases, the fringes first have an asymmetrical maximum-minimum form and then tend to a symmetrical minimum as the reflectivity increases to 60%, the minimum becoming sharper as the very highest (90%), reflectivities are approached. This implies that F is tending to $(2n+1)\pi$, approaching it, however, from values between $(2n+1)\pi$ and $2(n+1)\pi$ as the reversed sense of the asymmetry requires.

The rapid variation of F in the range of low reflectivities, and the colours which the metal films present, would appear to be related to the state of aggregation of the metal of the film, since these phenomena occur for a range of equivalent film thicknesses which are very small for explanations based on interference. The consideration of the very thin films of silver and of other metals such as gold, aluminium, copper and chromium using the reflected fringes as a means of observation will not be presented here but will be appended in the form of a publication³ since our present objective is to investigate the types of fringe which will be most useful in topographical studies of metals.

References - Chapter II.

- 1 M.Hamy. J.Phys.Rad.,5,789,1906.
- 2 J.Brossel. Proc.Phys. Soc.,59,224,1947.
- 3 J.Holden. To be published.

Chapter III

The Use of Reflection Fringes in Topographical Studies; The Choice of Reflection Coefficients.

From the experimental observations discussed in Chapter II, it was seen that when the reflection coefficient of the first surface exceeds 60% the reflected fringes present the visual appearance of fine minima against a bright background (e.g. Figure 9(b)), and a microphotometer is needed to reveal the slight asymmetry still present. In this range F is measured to an accuracy of $\frac{\lambda}{30}$ and for the range $0.6 < R_I < 1.0$ it is found to be equal to $(2n+1)\pi \pm \pi/10$. The measurement of F in this region of high first surface reflectivities is not capable of higher accuracy by the present method since the measured quantities are small, (being shifts of Δ_{max} & Δ_{min}), and in the equation in which they are to be substituted, $\frac{\partial I_{Rx}}{\partial \Delta} = 0$, as R_I & R_2 approach the value 1.0 small errors in the measured quantities cause large variations in the calculated values of F .

From the discussion on page 14, condition (c), it was seen that if the two conditions:-

$$\left. \begin{array}{l} F' \rightarrow (2n+1)\pi \\ R_1 \rightarrow 1 \end{array} \right\}$$

could occur together the maxima and minima in the reflected intensity distribution would tend to be superimposed, that is, an additional tendency towards sharpened fringes would be present, adding to the ordinary Fabry-Perot sharpening consequent upon the fact that $R_I \rightarrow 1.0$; It is observed experimentally that the reflected fringes at high reflection

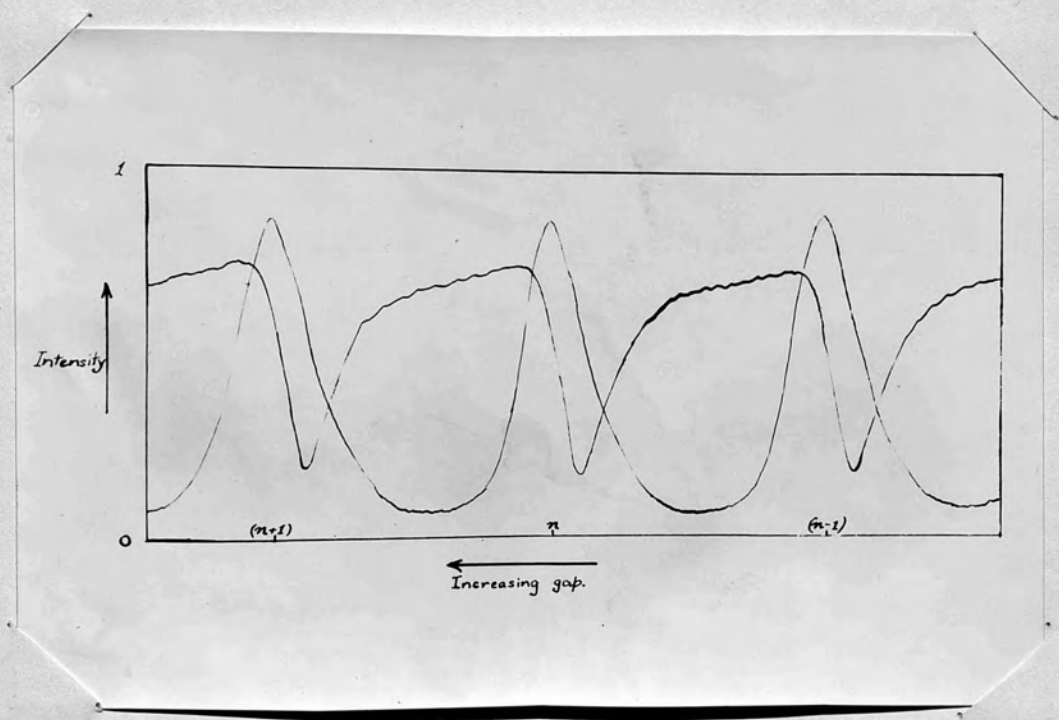


Figure 11.

coefficients become sharper than the accompanying transmitted system, whose sharpness is controlled by the function \mathcal{C}_Δ alone. Figure II shows a photostat copy of a microphotometer trace of reflection fringes where $R_I \sim 0.6$, and the movement of the maxima and minima towards superposition at $\Delta = 2n\pi$ is apparent. The accompanying transmitted system showing simple minima at $\Delta = (2n+1)\pi$ and simple maxima at $\Delta = 2n\pi$ is also shown. The traces are intended to show intrinsic shape of the fringes only and so the resolution of the photometer slit is not at its maximum, hence the lack of "graininess" in the trace; also the relative intensity levels of the two fringe systems are not corrected for plate response on this particular trace.

Thus in order to examine the sharpness and contrast of the reflected fringes in the range $0.5 < R_I < 1.0$, which is the range where the fringes are sharp enough for topographical work, we can take with good approximation $F = (2n+1)\pi$. Therefore the reflected intensity from a symmetrical ($R_I = R_2$), working interferometer in the high reflection range will be:-

$$(F = \pi ; r_1^2 = r_2^2 = R ; t_1^2 = t_2^2 = T ;)$$

$$I_{R_x} = R + \left\{ \frac{T^2 R + 2TR^2 - 2TR \cos \Delta}{1 + R^2 - 2R \cos \Delta} \right\}$$

The maxima occurring at $\Delta = (2n+1)\pi$ and the minima at $\Delta = 2n\pi$. By maxima in this high reflection range we will effectively mean the general background intensity which will be very closely the same everywhere except in the locality of the sharp reflection minima at positions given by $\Delta = 2n\pi$. (c.f. Figure II).

Minima: The minimum intensity in the reflected fringes, $(I_{Rx})_{\min.}$, is therefore:-

$$(I_{Rx})_{\min.} = R + \frac{RT}{(I-R)^2} \cdot (T + 2R - 2)$$

If there is no absorption in the silver film comprising the incident surface we can write:-

$$R + T = I$$

and the minimum reflected intensity in the case of no absorption, $(I_{Rx})_{\min.}^0$, becomes zero. If there is absorption defined by A, such that:-

$$R + T + A = I$$

the minimum reflected intensity, $(I_{Rx})_{\min.}^A$, becomes $A^2 R / (I-R)^2$, Thus:-

$$(I_{Rx})_{\min.}^A = (I_{Rx})_{\min.}^0 + \frac{R}{(I-R)^2} \cdot A^2$$

Therefore the minimum intensity in the reflected pattern is raised from its value zero, in the case of the ideal non-absorbing film, to the value $A^2 R / (I-R)^2$ when there is absorption defined by $R+T+A=I$.

Maxima: The maximum intensity, or background level, in the reflected fringes is:-

$$(I_{Rx})_{\max.} = R + \frac{RT}{(I+R)^2} \cdot (T + 2R + 2)$$

If there is no absorption we can write $R + T = I$, and the

maximum reflected intensity becomes:-

$$(I_{Rx})^0_{\max} = R + \frac{R}{(I+R)^2} \cdot (3 - 2R - R^2)$$

If there is absorption defined as before, the maximum reflected intensity for absorption A , $(I_{Rx})^A_{\max}$, is:-

$$(I_{Rx})^A_{\max} = R + \frac{R}{(I+R)^2} \cdot (3 - 2R - R^2 + A^2 - 4A)$$

Since typical values of A at the higher reflectivities employed in multiple beam interferometry with silver evaporated films are of the order of 0.05 , $A^2 \ll 4A$.

Therefore:-

$$(I_{Rx})^A_{\max} = R + \frac{R}{(I+R)^2} \cdot (3 - 2R - R^2 - 4A)$$

Thus:-

$$(I_{Rx})^A_{\max} = (I_{Rx})^0_{\max} - \frac{R}{(I+R)^2} \cdot 4A$$

Therefore when absorption A is present, defined by $R+T+A=I$, the maximum reflected intensity is decreased by an amount $4AR/(I+R)^2$.

The following Table, (Tolansky 1946), gives typical values of R, T and A for silver films prepared for use with the transmitted system of fringes.

R%	60	70	80	75	85	90	94	
T%	35.5	27	16.5	22	10.5	4.5	0.7	($\lambda = 5461\text{\AA}$)
A%	4.5	3	3.5	3	4.5	5.5	5.3	

The usefulness of the transmitted system is usually described by the reference to the fringe "half-width", or the reciprocal of the half-width, which is a measure of sharpness, and to the quantity ($I_{\max} - I_{\min}$), which is a measure of their visibility. Similar indices can be used to describe the reflected system at high reflection coefficients, Figure I2* illustrates these quantities in the two systems of fringes.

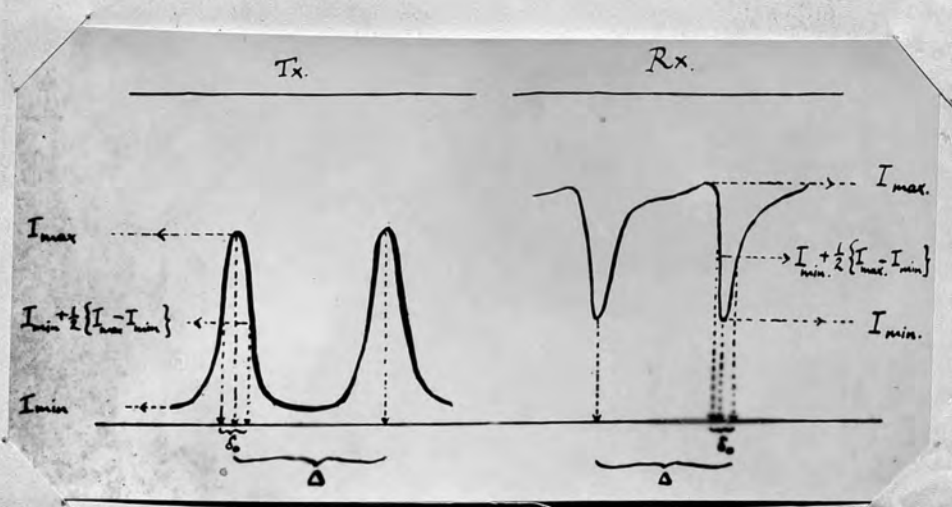


Figure I2.*

With the aid of the formulae deduced above we can compare the merits of the two systems of fringes. Figure I2 shows the values of $(I_{Rx})_{min.}$ & $(I_{Rx})_{max.}$ for the good practical values of R, T and A quoted in the preceding Table, in the curves marked I. While Figures I3 and I4 show respectively the "sharpness" and "contrast" of the reflected and transmitted fringes which would arise in an interferometer using these silverings.

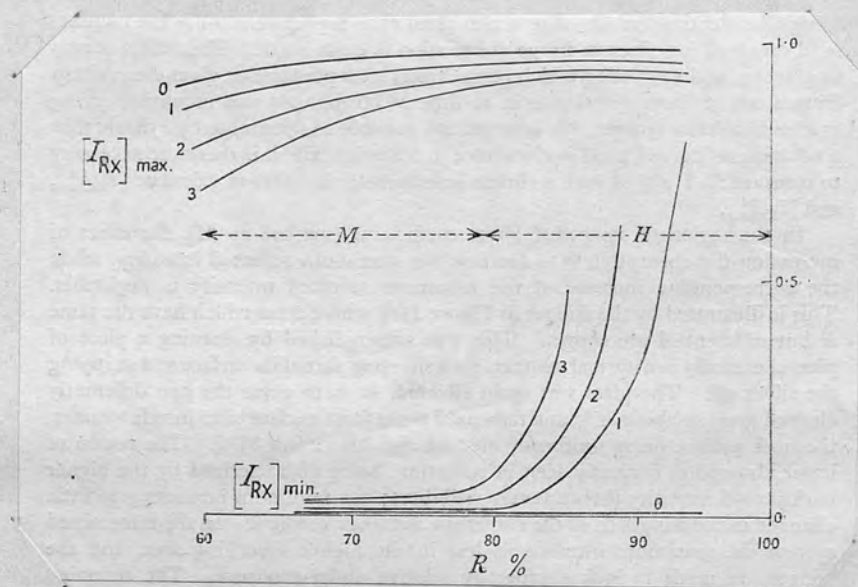


Figure I2.

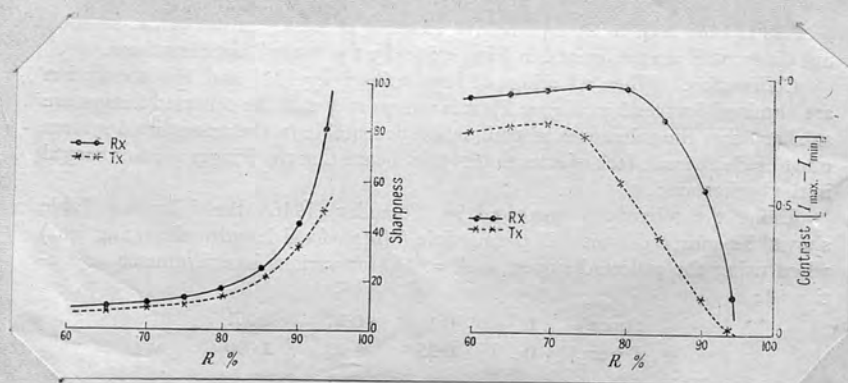


Figure I3.

Figure I4.

From the sharpness and contrast curves of the two systems the superiority of the reflected system for precision measurement is apparent. The preparation of the silver films for use with reflected systems, however, requires especial care as the following considerations will show. In Figure 12 are drawn two families of curves: the upper set shows the value of the maximum reflected intensity, $(I_{Rx})_{max.}$, for different values of the absorption A ; the lower set shows the values of the minimum reflected intensity for the same values of A . In each family the curve marked 0 shows the values of the quantities when the absorption is very small ~ 0.01 , the curve marked 1 shows the values of the quantities when A has the values shown in the preceding Table, and the curves marked 2 and 3 show the quantities when the absorption has values respectively 2 and 3 times these good practical values. In the region of high coefficients (marked as H), it can be seen that a slight increase in the value of A for a film of reflectivity 90% is very critical since it changes the fringes from a state of sharpness and good contrast to a condition in which the contrast is so poor that the fringes cannot be seen at all. For a film in a range of higher reflectivity the increase in A required for effective fringe obliteration is even slighter. In effect the vertical asymptote to the curves $(I_{Rx})_{min}$ indicates in its intersection with the axis of R the limit to the reflectivity useful when working with the reflected fringes arising from silverings prepared by such a process that the absorption is of the magnitude used in the drawing of the curves $(I_{Rx})_{min}$. It is not possible, as yet, to determine by eye whether a silvering will give a good performance in reflection, and it is therefore necessary to measure R , T and A with a simple

reflectometer in order to calculate $(I_{Rx})_{\max}$ and $(I_{Rx})_{\min}$. In practice, the effect of an increase in A is observed when a silvering, on preparation, gives clear sharp fringes which can deteriorate in as little as one hour to very bad visibility fringes. This is prone to happen when very high reflectivities in excess of 90% are prepared, with a relaxing of the conditions of cleanliness of the sub-strate on which the silver is deposited.

In the region of somewhat lower coefficients, (marked as M in Figure I2), the effect of increasing absorption is to decrease the maximum reflected intensity while the accompanying increase of the minimum reflected intensity is negligible. This effect is illustrated in Figure 9(c), where areas which have the same R but different A are shown. This was affected by cleaning a piece of glass in the normal chemical manner, then silvering part of the surface and stripping the silver off. The glass was again silvered so as to cover the two differently cleaned areas to about 75% reflectivity and then used as an interferometer front surface, the back surface being uniformly cleaned and silvered to about 82%. The fringes of Figure 9(c) result and one can pick out the region of lower absorption from observation of the reflected fringe system since it is characterised by the higher background intensity (hence better visibility); the minimum intensity is little changed in the fringes from the two areas. In the transmitted ^{system} the effect of increased Absorption can just be seen in the decreased maximum intensity whereby the fringes, by relative under exposure, are made to look slightly sharper in the area of higher absorption. In the Figure there are also shown areas of the same A but different R and these are recognised by the step in the fringes marking the boundary between them consequent upon the differing thicknesses of silver used in the two areas to achieve the different reflection coefficients.

It is important to note that when silverings of high reflectivity ($\sim 90\%$), and low absorption are obtained (curves I of Figure I2), the reflected fringes are very sharp and the tolerations in collimation acceptable in the transmitted system must be decreased. Lack of attention to this means that the fringes are submerged in the background. Using the tolerances of fringe degeneration found acceptable in transmission work, (Tolansky 1946), the following Table shows the source diameter permissible, (D), with a 10cm. focal length collimating lens, when using the reflected system at $R = 90\%$ for various interferometer spacings, t.

t (mms)	1	0.1	0.01	0.001
D (mms)	0.1	0.35	1.00	3.000

Although it is desirable to have high reflecting coefficients, within the limits discussed in the preceding pages, when using the reflected system of fringes in surface studies, cases will arise when the back surface of the interferometer, which is the surface under examination, will not be coated with a highly reflecting silver film since the several techniques by which this is achieved may influence undesirably the surface structure. In these circumstances, the natural reflectivity of the surface under examination will be used and will, in the case of many metals, be reasonably high, although not quite as good as a silvered surface.

The effect of having R_2 , the reflectivity of the back surface of the interferometer, smaller is to cause the shape factor σ_{Δ} to have less rapid variations about

$\Delta = 2n\pi$, and to decrease the value of the magnitude terms upon which it operates, in comparison with the background term R_I , as the expression for the reflected intensity from an asymmetrical interferometer ($R_I:R_2$) shows:-

$$I_{R_x} = \left\{ R_I + \frac{T_1^2 R_2^2 + 2T_1 \sqrt{R_1 R_2} \cos(\Delta - F) - 2T_1 R_1 R_2 \cos F}{1 + R_1 R_2 - 2\sqrt{R_1 R_2} \cos \Delta} \right\}$$

The effect of this is loss of contrast and sharpness. However, by decreasing R_I to the range of values 50-70% the asymmetrical fringes can be usefully employed since the sharp side of the fringe can be used for measurement while the contrast is excellent. Even with R_2 as low as 30% the use of the asymmetrical fringes will allow quite accurate measurements of topography to be made. For instance, in the range of asymmetrical fringes it is found that, for typical silverings, when R_I is about 55% the minimum intensity within the fringes in reflection is close to zero. This allows a high degree of over exposure when photographing the fringes and, although the fringes are actually asymmetrical, a final image may be obtained which resembles a simple minimum on a uniform background of a sharpness resembling the fringes from 80% silverings.

With a view to applying the reflected fringes to a study of metal surfaces we may sum up their characteristic^s or reflectivities greater than 90% the fringes are sharper than the corresponding transmitted fringes but their visibility is critically dependent upon the absorption in the silver films deposited to form the reflectors; collimation conditions are strict. Complications of the simple interference relationship due to focussing

defect and large wedge angles are immediately obvious in the appearance of the fringes, and one can avoid the errors that creep into transmission work if high precision measurements are attempted without sufficient attention to these factors. The results and observations apply to the reflected fringes of equal chromatic order which obey the same fundamental formula, $n\lambda = 2t \cdot \cos \theta$, and to Fabry-Perot fringes.

Apart from the use of high reflectivities an important part is played in applied work by the transmission-like maximum fringes arising at a low critical reflectivity. With some metal structures, e.g. twin bands, the attempt to use low order fringes is sometimes rendered impossible by the large surface movements occurring, the high reflectivity fringes in such cases show complex maxima and minima similar to those illustrated in Figure 5(b). In such a case the lowering of the reflectivity of the reference surface to the value for maximum type fringes gives an intensity distribution such that the background intensity between fringes is too low to record the subsidiary fringes at normal exposures. We must remember that the distance between such fringes is not $\lambda/2$, but the correction is generally small and for angle measurements is negligible. This type of fringe is used extensively in the study of twinning, c.f. Ch. VII et seq.

References Chapter III.

- P. Rouard. *Ann. Phys.*, 7, 291, 1937.
 S. Tolansky. *Proc. Phys. Soc.* 58, 684, 1946.

Chapter IV

The Use of Reflection Fringes in Topographical Studies; New Criterion of Resolution.

In the foregoing, we have discussed how the reflected interference fringes from a wedge interferometer of optimum wedge angle and gap and whose surfaces are silvered to certain conditions of reflectivity and absorption, may be of the form of very sharp symmetrical minima such that the fringe thickness is less than $\frac{1}{30}$ th. the distance between successive orders. It is now proposed to substitute, in place of the silvered surface forming the back surface of the interferometer, a metal surface possessing surface structure of the kind illustrated in Figure I. The reflected fringes arising from the interferometer are to be imaged and used for measurement of the surface structure. In ordinary usage, the theory of the microscope reveals the essential need that the objective lens should be of adequate aperture to collect the diffracted beams from the observed structure and leads to the Rayleigh criterion of resolution whereby two points of high contrast are regarded as resolved when their diffraction patterns do not confuse to more than a certain degree. In our new method of observing microscopic detail, our image is a sharp interference fringe, giving us information about the relative heights along a line direction across the metal surface, and it will be in the factors governing the degeneration in sharpness and exact focus of the sharp fringe that the resolution limit of the new method will be expressed. We will therefore investigate the effect of structure of the magnitude shown in Figure I, upon the optimum conditions of wedge angle and gap, and of illumination, in a manner somewhat as follows.

It will be assumed that the observing lens is quite adequate to collect all the multiple beams going to form the fringe intensity distribution on the zero order Feussner surface. That is, as illustrated in Figure I6(a), the n^{th} reflected beam will be making an angle $2n\epsilon$ with the directly reflected beam and the aperture of the observing lens, θ , will be such that $\theta \geq 2n\epsilon$.

Consider then a surface detail consisting of a small sloping step as shown in Figure I5. A section through the step at right angles to its length is shown in (b), while (a) shows a perspective view with the upper reference surface, (the incident surface of the interferometer), orientated at a small angle β to the plane OXY, which is the plane of the metal surface. The interference fringes arising are shown in (c).

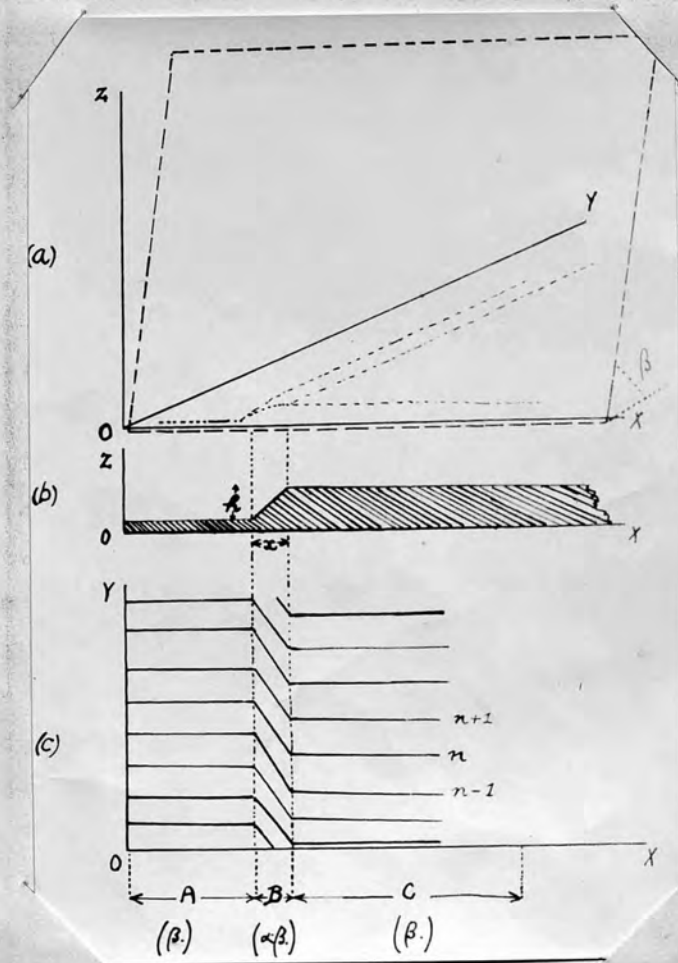


Figure I5.

In the regions marked A and C, the wedge angle is β ; while in the region marked B the angle is such that the slope in the direction OY is β and in the direction OX is α such that $\alpha = \tan^{-1} \frac{h}{x}$. We have seen however, p.15, that for a simple fringe form the wedge angle ϵ must be such that the phase lag terms, $\left\{ n^3 \frac{8\pi t \epsilon^2}{3\lambda} \right\}$ must be small compared with $n\delta$. If they are appreciable the sharp fringe degenerates into multiple maxima and minima, c.f. Figure 5(b), and precise measurement becomes impossible, since the fringes have lost the property of sharpness even though they are accurately focussed. Taking values $h = 1000\text{\AA}$; $x = 1\text{cm}$; then $\alpha \sim 0.1$ radians, about 5° , and for our usual values of n, δ the terms $\left\{ n^3 \frac{8\pi t \epsilon^2}{3\lambda} \right\}$, are excessive, and for these values of the step size the fringes in the vicinity of the step are confused and the detail is to all purposes presented as a break in the fringes but in a characteristic manner, not to be confused with the fringe break from a precipitous step, since the broken ends of the fringes cannot be joined by a line at right angles to them.

We must therefore lay down a working tolerance to the size of the terms $\left\{ n^3 \frac{8\pi t \epsilon^2}{3\lambda} \right\}$. Taking working conditions to be such that typically:-

$$n \sim 30 ; t \sim 10\lambda ; d \sim 20\pi ; \lambda \sim 5 \cdot 10^{-5} \text{ cms.}$$

Then it is found that a suitable tolerance is such that :-

$$n^3 \cdot \frac{8\pi t \epsilon^2}{3\lambda} \ll \frac{n\delta}{25} \quad \dots\dots(I)$$

Substituting the working values we find that the maximum wedge angle formed by local detail must not exceed 0.006 radians, thus

$$\underline{\epsilon_{\max} \quad 0.006}$$

From this value of ϵ_{\max} we can calculate the effective depth of focus of the fringe system, that is, recalling the formula of page 17, the amount we can focus on either side of the surface F⁰ before the fringe distribution degenerates too much. It will

be necessary to again take the toleration used in equation (I), thus:-

$$n^2 \cdot \frac{4\pi X \epsilon^2}{\lambda} = \frac{n \cdot d}{25} \quad \dots\dots(\text{II})$$

Substituting our typical values, including $\epsilon=0.006$, we find the limit to X to be 120λ , thus:-

$$\underline{X_{\max} \sim 120\lambda}$$

Thus we can write the effective depth of focus of the fringe system as 240λ .

From this value we can calculate the toleration in the collimation of the light incident upon the interferometer. We know, (c.f. p.18), that the Feussner surface for the light incident at angle ϕ is distant an amount "d" from the Feussner surface for the light incident normally such that:-

$$d = \frac{t}{e} \cdot \sin \phi \quad \dots\dots(\text{IV})$$

Substituting our value from the depth of focus calculation for d, and our other typical values we find the collimation toleration to be:-

$$\underline{\phi_{\max} = \sin^{-1} 0.12}$$

Further; we have to restrict this maximum allowable value of ϕ a little more since it has been pointed out^I that an angular deviation ϕ from the normal produces a fringe broadening "dn", such that $dn=2t/e \sin^2(\phi/2)$. Tolansky suggests a tolerance in dn of one fifth the half width of the fringes, which for reflectivities of 90% gives $\phi^2 = \frac{3.4 \times 10^2}{t}$

Inserting our typical values gives $\phi = .02$ radians. From this maximum value of ϕ we can derive the size of the aperture in the collimating system by substituting in the equation:-

$$\sin \phi = \frac{a/2}{f}$$

where "f" is the focal length of the collimating lens in the

I Tolansky, S.; Proc. Phys. Soc. 58, 654, 1946.

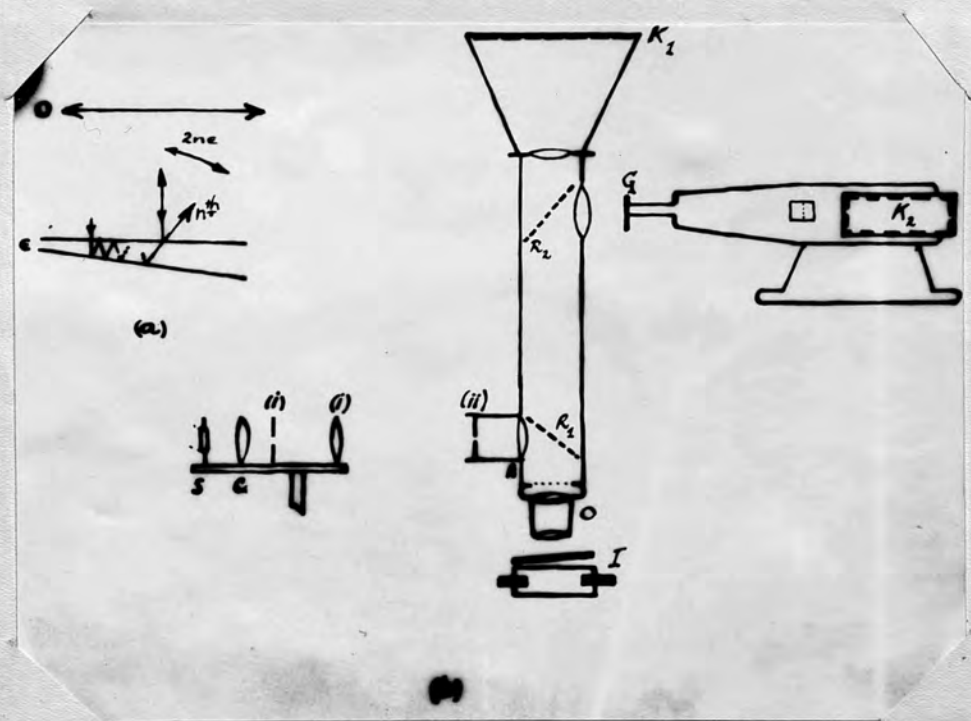


Figure 16

illumination system, which, for metallurgical work is generally the microscope objective (c.f. Figure I6 (b)), so we can take a typical value of 12mm. for f . Thus:-

$$\underline{a \sim 2\text{mm.}}$$

In Figure I6(b) therefore the size of the image of the aperture (i) in the back focal plane of the microscope objective must be less than this value calculated for "a".

Returning to our value for ϵ_{max} , we can now calculate the numerical aperture of the objective such that it will be able to satisfy the condition, mentioned at the outset, of collecting all the multiple beams going to form the fringe intensity distribution on the zero order Feussner surface.

$$2n\epsilon_{\text{max}} = \sin\theta = \text{N.A.} \quad \dots\dots(\text{VI})$$

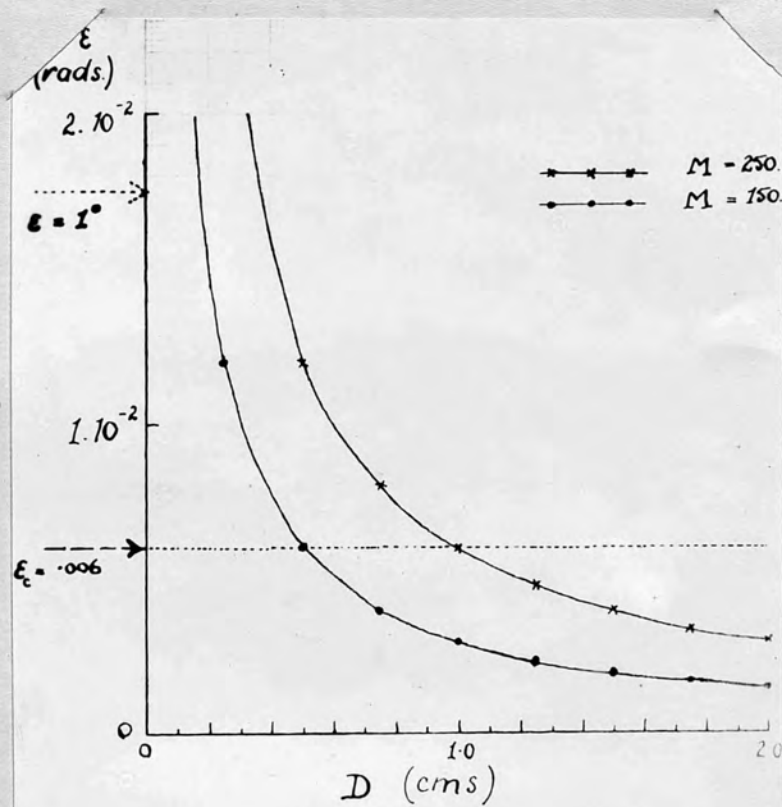
Substituting our values we obtain the minimum numerical aperture of 0.35.

$$\underline{(\text{N.A.})_{\text{min}} = 0.35}$$

Thus any lens of numerical aperture greater than this value will perform adequately as an objective, it will also have to possess a working distance such that the reference flat, or first surface of the interferometer, will be able to be positioned between the front lens surface and the metal surface to be examined. In practise this means that the 12mm. lens is the most powerful lens in the generally available range for our purposes, they have N.A. 0.65.; while the 16mm. lenses N.A. 0.30 are also used for general work when the highest available resolution is required. It will be appreciated

that we can use as much magnification at the eyepiece as we wish, there being no empty magnification in the usual sense, in practice the fringe pattern is enlarged for ease of vision and typical total magnifications in the superficial plane of X250 are quite adequate. Although our resolution criterion is stated in the form $\epsilon_{\max} = 0.006$ radians, we may obtain some idea of surface resolution by imagining a sloping step say, 250\AA high, then it would have to extend $1/250\text{mm}$. in its rise in order that the fringe may continuously contour it. From this sort of sloping step to a detail which we may think of as precipitous, then all depends upon the height of the detail, and we cannot generally state any linear distance as the limit of resolution. The way in which the fringe ceases to contour the surface in the vicinity of say, a slip band is instructive and the elucidation of the fine structure can be approached by several methods to be discussed presently. The enlarged image of the fringe system can be checked to see if the wedge angle exceeds the maximum allowable for exact measurement on the fringes, by means of the graph shown in Figure I7. The fringe spacing between orders is plotted against the wedge angle to cause it for magnifications of 150 and 250. The maximum value of ϵ is drawn in, thus we see that for magnifications between the values mentioned we can read off the minimum fringe spacing that must be present on our image if we intend to use it for precise measurement. It may be mentioned that the limits discussed above are inclined to be on the side of rigour and for much general work we can still obtain satisfactory results when they are slightly relaxed.

Diffraction taking place at the metal surface is not seriously disturbing in the case of isolated simple details since the diffracted beams, after being multiply reflected, have to traverse the incident surface silvering, which is generally greater than 80% reflectivity, and the intensity of the beams is thus reduced from their initially small value to a negligible one.



Graph of:- $\epsilon = \frac{\lambda}{2} \frac{M}{D}$

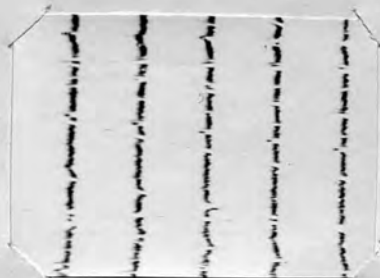
Figure I7.

Before proceeding to examine diffraction effects further it will be advantageous to refer to Figure 16(b) which illustrates the microscope system in use. The layout results from the circumstance that we have at our disposal two ways of dispersing the interference fringes arising from the interferometer I. We may employ an initial wedge angle, (the angle β of Figure 15), and thus disperse the fringes in the plane of the interferometer surfaces such that they run at right angles to the direction of the general wedge angle β . Alternatively we may disperse the fringes with the aid of a spectrograph, the Feussner surface being imaged on the spectrograph slit, G, and using a white light source instead of a monochromatic one we obtain in the focal plane of the spectrograph, K_2 , fringes possessing the characteristic of constant $\frac{t}{\lambda}$, for each order as compared with constant t for the fringes localized on the wedge when employing the angle β . It is sometimes inconvenient to try to achieve a constant general wedge angle β over all the field of view -- a condition necessary for constant dispersion of the fringes -- so the spectrograph fringes, known as fringes of equal chromatic order (Tolansky 1946), or channeled spectra (Rouard 1937), are employed since in their case we are only imaging a slit image of the interferometer surface, or more strictly the Feussner surface, thus the value of β can be zero. The illumination system of Figure 16(b) is as follows. The condenser C images the monochromatic or white light source S onto the iris (i). This iris is imaged by means of the lens (1), in conjunction with lens A, onto the back focal plane of the objective O, thus the interferometer is illuminated with a near parallel beam. The iris (ii) is imaged by Lens A and the objective onto the interferometer surface to restrict the illumination to the field of view only. R_1 is a 50% reflector as is R_2 . The fringes of equal thickness, suitably magnified are observed at K_1 while the fringes of equal $\frac{t}{\lambda}$ are observed at K_2 . The illumination train, S:C:Iris(i):Lens(1), is adjustable as a unit for different objectives.

In order to illustrate experimentally the resolution limits discussed in the foregoing pages and to show how the particular surface structure or feature under observation sometimes adversely and sometimes favourably affects the reliance we can put into our measurements on fringes, we can briefly mention the following observations on different surfaces.

A. Surface Finish.

In figure A are shown Fizeau fringes from a steel surface which was ground with successively finer abrasives. The fringes show the size of the scratches produced by the final abrasive, (*700 Al₂O₃ grit.*), along with isolated deeper and wider scratches from earlier abrasives ^{used} in the process of grinding down to an over all optical plane surface, and thus give a good method for grading the surface roughness of say, engineer's gauges. However in such a complex structure quite a large amount of light goes into the diffracted orders, in contrast to the case of the single isolated surface step, and this appears on the side of greater thickness in the fringe pattern giving the fringes a "wing" on the side greater "t". This causes the depth of the individual surface irregularities as revealed by optical interference to be slightly greater than the measure given by a stylus type instrument, also it gives the shape of the irregularities a false sharpness. Within these extra limitations imposed by this type of structure it is seen that our theoretical resolution limits are followed.

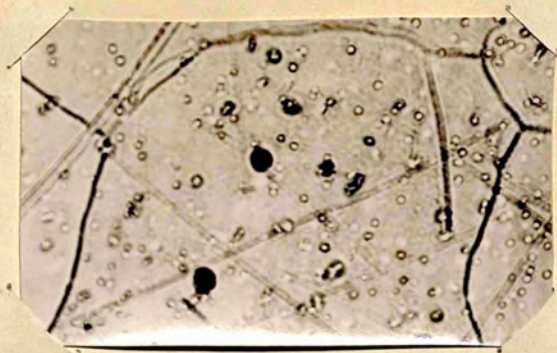


X 150

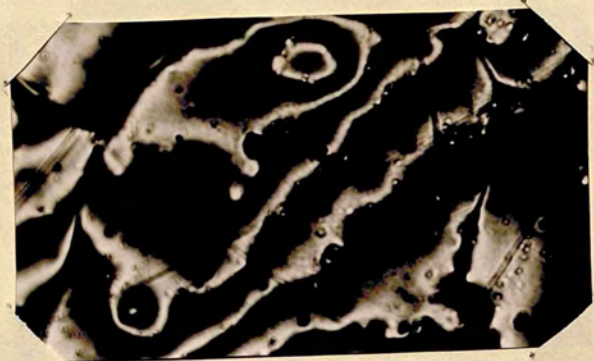
Figure A

B. Etching of Grain Boundaries.

In contrast to the complex structure discussed in A, we now take an isolated surface feature, the grain boundary depression as developed by electrolytic etching or by thermal methods.^I Figure B1 shows the boundary between two grains of Aluminium in a specimen polished and etched in a Perchloric acid/Aceatic acid solution. The ordinary micrograph shows the boundary as a dark line, the asymmetric fringes give an intensity distribution over the surface and indicate the V-like profile of the boundary groove which is then examined with the very sharp fringes to give an accurate profile. We can follow the fringe, clearly defined, to the apex of the "V" which is the bottom of the boundary groove, because in this case the angle which the groove sides make with the reference surface of the interferometer never exceeds the permissible maximum of about one hundredth of a radian which was the limit arrived at for sharp fringes, c.f. Page 40. It is therefore no surprise to measure the angle between the two sides of this particular groove at its vertex as being $179^{\circ} 24'$. The interferometric method will be expected to fail when the angle at the bottom of the groove is other than close to 180° . This is the case as shown in Figure B2, where a boundary between grains in a specimen of Silver is shown after being heated at $800^{\circ} C$ for a period of ten hours in a fused silica boat. The angle between the sides of the groove is such that the interferometer wedge angle is very large and the interference fringes become multiple as in the case of Figure 5(b), page I7, and all definition in the region of the groove is lost. It is, however, clearly shown where the large majority of the material from the groove has gone to, in the "hump" which the fringes show on each side of the groove. This is compatible with the mechanism of surface mobility.



(i)



(ii)



(iii)

Figure
B1
(X200)



Figure
B2.
(X200)

C. Polish.

Figure C shows a heavily polished Tungsten surface in the middle of which is a pit made by a spark, the specimen being one of a pair of "contacts". From the indicated magnification we see that the sides of the pit slope down at an angle more than ten times our permitted maximum for general conditions. The fact that in this particular case we do get a fringe of some definition is due to the circumstance that, "t", the optical separation of the interferometer in the vicinity of the pit is very small indeed due to reference surface being forced against the tungsten surface with some force. Some idea of this is perhaps indicated by the broad dispersed fringe of extremely low order within which the pit fringes are formed. Examination of this broad fringe shows that it has a "mottled" appearance and this appearance is found to be characteristic of polished steel too, particularly if the polishing process is continued for a prolonged period.

Interpretation of the intensity distribution within a broad dispersed fringe has been carried out by Tolansky and Wilcock² during the examination of a diamond surface. In the same way we have in the present case, due to high magnification rather than high dispersion, a fringe within which there is a sensitive relation between intensity and relative phase. Interpreting this as we can do quantitatively knowing the reflection coefficients of the interferometer surfaces leads us to the view that the highly polished layer

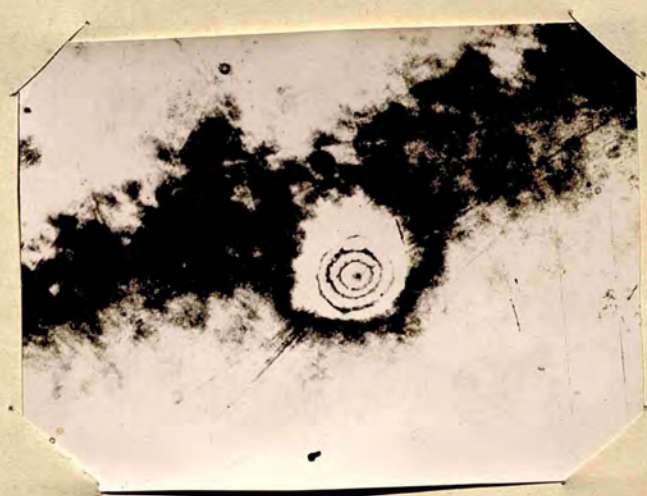


Figure C.
(X250)

2. Tolansky & Wilcock. P. R. S 191:182; 1947.

has a gently undulating topography, the "waves" being of the order of 250Å in amplitude and 10^{-4} cms. in wavelength. A microphotometer trace indicated smooth changes of intensity within the fringe leading to the inference that the height changes were particularly continuous. This characteristic of the polish structure³ is at the basis of our ability to interpret the fringe system to a greater degree than is indicated in a general statement of resolution limit.

The particular surfaces which have been illustrated give an idea of the way in which the methods of interferometry will fare when applied to deformation features of metals and illustrate the compromise between superficial resolution and resolution in depth which must be made when optical methods of rendering small scale details are attempted.

The processes of polishing are most important for the study of metals and of recent years electropolishing has been an essential feature of specimen preparation. The successful techniques⁴ evolved have been in many important cases, peculiar to the particular metal involved. In the course of the present work fairly large areas, (1 cm. sq.), of a specimen were required to be completely flat as well as free from local imperfections. The fact that the specimen was immersed in a liquid for electropolishing made this former requirement hard to achieve. However the technique of electropolishing offers many variants of specimen location and procedure and the requirements of interferometric type metal surfaces will ^{flatness} ~~and the~~ ^{it is thought} be attained for each metal. It is of some interest to note

3, Thompson. *P. Nature* 121, 1931, 563.

4, Lacombe & Beaujard, *Rev. Metall.* 53, 216, 1948.

that during the process of electropolishing the type of surface feature formed very often by the electrochemical action is ideally suited in form to interferometric investigation. For example, Figure D shows the surface of an Al specimen immersed for two minutes, after grinding to 3/0 emery, in a bath of perchloric acid/Acetic anhydride solution, the current density being about twice that used for polishing. The rounded off non-precipitous hillocks are accurately conoured by the interference fringes.

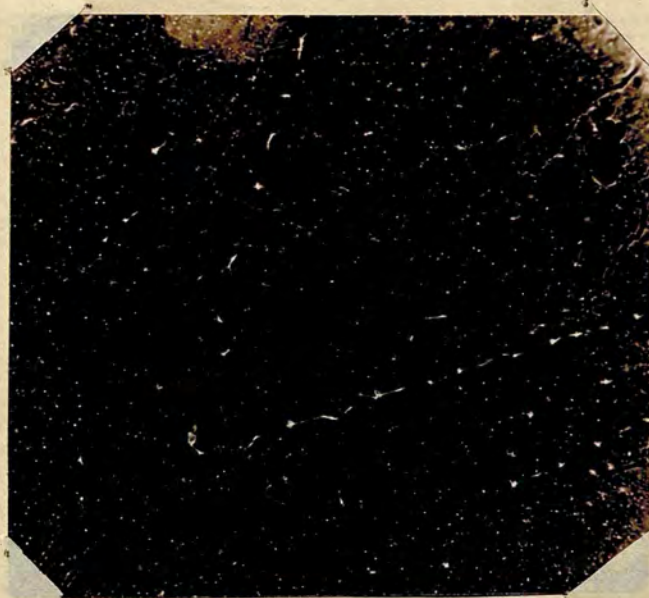
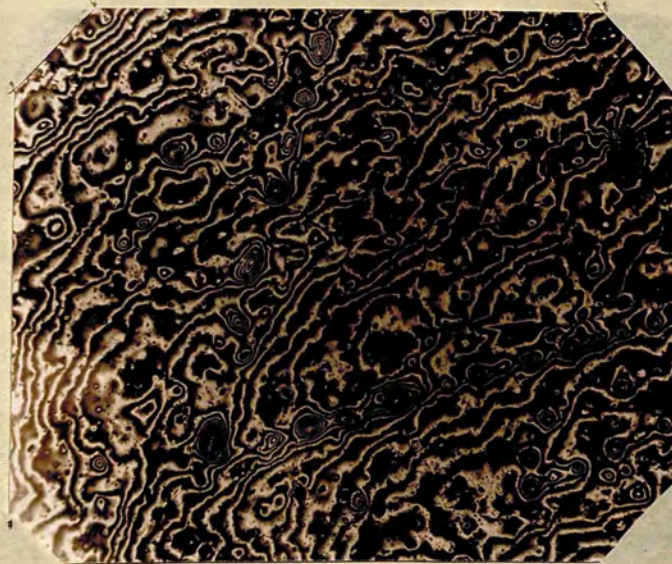


Figure D.

 $(\times 100)$ 

Chapter V.

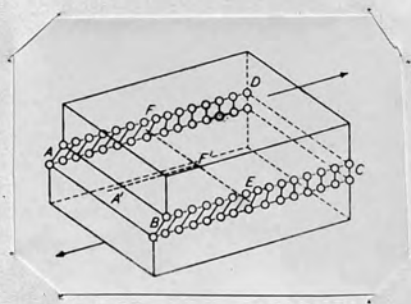
Introduction to the Experiments on Twinning and Slip.

Our understanding of the ways of deformation of a crystalline solid has had contributions from many widely differing scientific studies. In addition, the field of study has been influenced by the well developed technologies which have been built up around the specially important industrial substances such as metals. It is thus characteristic of the subject that, at times, progress has seemed to take place comparatively slowly due to the need to carefully assess the experimental evidence. Similarly the emergence of general underlying physical ideas has been faced with the task of satisfying the requirements revealed by the experiments of X-ray Crystallographers, Metallurgists and Chemical Crystallographers, which have frequently seemed conflicting.

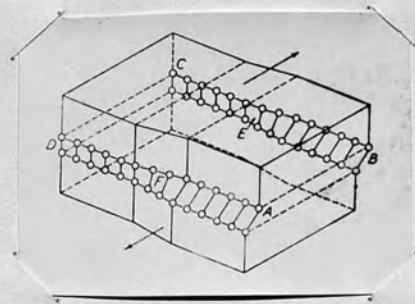
The physical approach, which aims at constructing a theory of the mechanics of the atomic movements involved in plastic deformation, is now being developed and it has become clear that the link between the atomic structure of metals and their crystallographic plastic properties is a kind of crystal lattice defect originally referred to, from its geometry, as a Dislocation. The theory^I as conceived by Taylor, Polanyi and Crowan at about the same time, was an attempt to explain the remarkable properties of plastic gliding displayed by single crystals of metals and of ionic crystals such as rock-salt. The idea that plastic gliding was due to the-

the passage of dislocations through a crystal was fruitful then in explaining the very small stresses required to initiate the glide deformation and also the increased resistance to glide as the deformation proceeded. The elaboration of these ideas of the types and properties of dislocations²; their interaction among themselves, the stress required to move an individual dislocation, the way in which they form stable assemblies, -- have lead to very acceptable theoretical pictures of how other phenomena of the crystalline lattice can be imagined as taking place. At the same time the theory has brought into prominence new experimental aspects of the well-known deformation phenomena, and stiffened up older control conditions. It is thus against the background of this physical theory of Dislocations that we introduce the present study of slip and twinning, using the methods of surface interferometry; while at the same time we bear in mind the difficulties of generalization shown to exist previously in other experiments in this field.

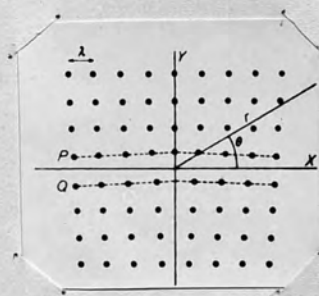
The types of dislocation arise naturally from the crystallographic basis of plastic deformation. Figure I8 (after Cottrell), shows in (a) a crystal possessing a glide plane ABCD, region ABEP has slipped in the direction A'F', region FECD has not slipped thus giving rise to the line EF perpendicular to A'F', known as the dislocation line. In (b) of the figure the structure of this type of dislocation line is represented, we see that atoms in the upper half crystal P are compressed along the slip direction and those in the lower half Q are extended. Such an imperfection was conceived by Taylor^I in his theory of plastic deformation; a second type, in which the dislocation line was parallel to the direction of displacement was introduced by J.M. Burgers³, and this type is visualized with the aid of (c) of Figure I8. Here a part



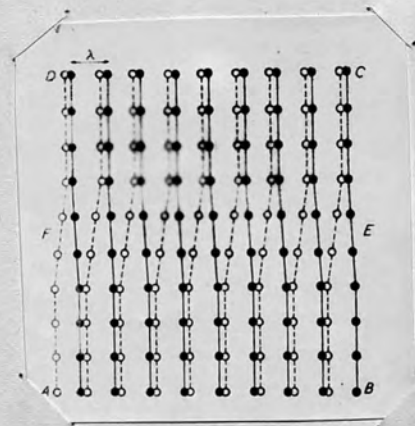
(a)



(c)



(b)



(d)

Figure I8

of the crystal ABEF has slipped in the direction EF while the rest FECD has remained unslipped. The line EF constitutes a "screw" dislocation and the atomic arrangement in its vicinity is represented in (d), which is a plan view of the atomic planes which slip over each other, the full lines representing the atoms of the upper plane and the dashed lines the atoms of the lower plane.

These dislocation boundaries are consistent with a view of a crystal which takes the atoms to be elastically coupled, subject to thermal vibrations and local sources of irregularity, and which will therefore tend to make the forces acting over a glide plane non uniform. This effect will thus spoil the perfection of crystallographic movement observed to account for the over-all plastic deformation of a crystal, and this local spoiling can be considered, by virtue of the crystal's discrete atomic structure, in terms of these two simple types of boundary between slipped and unslipped regions of the glide plane. Since a dislocation cannot be pictured to end within a crystal, i.e. the end of an edge or Taylor dislocation necessarily defines the start of a screw dislocation within the body of a crystal, then we take the general form of dislocation to be of a compound type, composed of segments of edge and screw dislocations, and forming closed loops within the crystal or alternatively having their two ends on the crystal surface. Metals possess less simple lattices than the cubic one used in the representation above but the detailed form of the atomic arrangement at the centre of the discontinuity is found to play a less important role in the theory than the stress distribution around a dislocation at distances from its centre large compared with the atomic spacing.

Regarding the experimental features of the phenomenon of glide, a comprehensive review⁴ of the crystallographic elements involved shows that in the case of single crystals the glide plane would seem to be less fundamental than the glide direction. For example, even with hexagonal crystals possessing a unique axis of symmetry where slip normally takes place on the basal planes, the influence of higher temperatures may promote slip on the pyramidal $(10\bar{1}1)$ or $(10\bar{1}2)$ faces; while with Aluminum, higher temperatures allow glide on cubic faces as well as on the normally active octohedral planes. However the glide always takes place in the direction of the most closely packed line in the lattice in the case of the hexagonal, face centred cubic, tetragonal and rhombohedral lattices. This is also true of the body centred cubic lattice with, in their case, the further classification of observations that the glide plane in operation is determined by the the ratio of the temperature of the deformation to the melting point of the crystal concerned. As this ratio increases the slip is observed to take place on the $11\bar{2}$ planes then on 110 and finally on the $12\bar{3}$ planes.

A great deal of observation⁵ has been carried out on the surface markings produced by this crystallographic activity, and it is not surprising that the markings, which are given the general description "glide bands", show a diversity of appearance when it is recalled that the conditions of deformation can be so widely varied. Apart from variation of the temperature at which the deformation is carried out the rate of strain of the specimen can be changed as is emphasised by the refined experiments⁶ on the phenomenon of creep. The important results of these experiments has lead to a dynamical approach⁷ to the glide process in which the time rate of strain and not the strain itself is measured as a function of stress. It is experimentally observed that the time rate of strain depends upon the temperature of the deformation and upon the "state of strain hardening" of the specimen; a factor

a factor which brings in the whole thermal and strain history of the crystal under examination. Such an approach has been very successful in describing the macroscopic deformation of metal crystals under diverse deformation conditions of strain rate and temperature and in conjunction the theory of dislocations has been developed to give a theoretical picture of the atomic processes involved.

Assumptions have been made in this development of the theory about the "sources" of dislocations within a real crystal and about the "obstacles" the moving dislocations meet with during the course of deformations. Further detailed assumptions are involved in theories put forward⁸ to account for the facts of gliding but these two main points are always involved and in this connection it may be of value to look once more at the structure of glide bands and to again make measurements upon their spacing, their fine structure, and in addition upon the "height" of the bands, i.e. upon the amount of movement along the glide plane, and upon the surface bending or tilting which may accompany the concentration of dislocations in an active glide band.

Recent electron microscope studies⁹ have been made, in the case of aluminium, upon the form of glide bands and they have shown a fine structure within the band and measured the height of the band. Although the fine structure brought to light in this particular case is too small to be revealed by an optical method, such a method may still be of use in that it allows continuous observation of the development of the glide band for a range of loads as opposed to the static conditions of the electron microscope type of observation. In particular much of physical interest resides in the very early stages of nucleation and growth of the band when the limitations of an optical microscope modified to work in accordance with the principles described in the previous chapters will be least felt.

Although optical methods must necessarily fail to give information about surface structures smaller than the order of the wavelength in use for illumination, in the direction parallel to the surface, there is one respect in which the microscope is found lacking before this limit is reached. This occurs with a surface structure which may be made up of domains tilted slightly with respect to each other. When this tilt is fairly large as in a polycrystalline creep specimen, where the grain boundaries have allowed rotation of the grains at high temperatures¹⁰, the microscope image does indicate the effect by the a difference in the amount of light thrown in to the microscope objective from each grain. For small relative tilts and small domains this is a feeble effect and the tilting in these cases can then be revealed and accurately measured by the interference microscope which is in effect a micro-goniometer, suited to a specimen possessing one main face on which are located small tilted areas. We are led to include this type of observation from a consideration of the lattice bending which a concentration of dislocations necessarily involves and which in suitable cases will be revealed on a surface of a crystal. In addition the several types of mosaic concept invoked by crystallographic theories would involve this type of surface structure. For example, in the study of the properties of assemblies of dislocations J. M. Burgers¹¹ brought forward the concept of a domain, free from stress in its interior and bounded by dislocation transition surfaces. This circumstance it is suggested can arise when the domains have reached dimensions of the order of 10^{-4} cm. and this type of domain plays an important part in the Burger's theory of the mechanism of the formation of slip bands.

Finally the importance of goniometric measurement is seen in the study of the surface movements involved in the apparently neglected phenomenon of twinning. Although X-ray studies have indicated the final atomic positions in a twinned region of a metal crystal, direct measurement of the surface tilts of a metal crystal at the boundary of a twin region may assist in understanding how the twin movement takes place. In addition the optical approach emphasises the characteristic way in which a twinning movement spreads throughout a crystal and the secondary effects which accompany the damping out of a twinning movement.

References -- Chapter V.

- I Taylor, G.I. Proc. Roy. Soc. A145, 362, 1934.
Crowan, E. Z. Phys. 89, 605, 1934.
Polanyi, M. Z. Phys. 89, 660, 1934.
- 2 Report of Conference on Strength of Solids, The Physical Society, 1948.
- 3 Burgers, J.M. Proc. Kon. Acad. Wet. Amst. 42, 1939.
- 4 Andrade, E.N. da C. Proc. Phys. Soc. 52, I, 1940.
- 5 Kuhlmann, D. Z. Metallkunde, 41, I29, 1950.
- 6 Andrade & Chalmers. Proc. Roy. Soc. A138, 348, 1932.
- 7 Crowan, E. Proc. Phys. Soc. 52, 8, 1940.
- 8 Frank, F.C. Strength of Solids, p.46, Physical Society 1948.
- 9 Heidenreich & Shockley. J. Appl. Phys. 18, 1029, 1948.
- 10 Hanson & Wheeler. J. Inst. Met. 55, 1931, 229.
- 11 Burgers, J.M. Proc. Kon. Akad, Wet. Amst. 42, 1939.